DÉVELOPPEMENT D'UN NOUVEAU CONCEPT DE TEST DE RÉPONSE THERMO-HYDRAULIQUE POUR ÉCHANGEURS DE CHALEUR GÉOTHERMIQUES VERTICAUX

Mémoire

JEAN ROULEAU

MAÎTRISE EN GÉNIE MÉCANIQUE
Maître ès sciences (M.Sc.)

Québec, Canada

Résumé

Il est important de connaître la conductivité thermique du sol ainsi que l'amplitude et l'orientation de la vitesse des écoulements souterrains lors du dimensionnement d'un champ de puits géothermiques. Ce mémoire présente la méthodologie et les conclusions d'une analyse numérique d'un nouveau concept de test de réponse thermique (TRT) pour échangeurs de chaleur géothermiques verticaux. Cette configuration de TRT permet de mesurer à la fois les propriétés hydrauliques du sol et ses propriétés thermiques. Le but premier du mémoire est de vérifier la validité du concept pour ensuite développer une méthode de résolution permettant d'estimer, à partir de la réponse thermique lors du TRT, la conductivité thermique du sol ainsi que la norme et l'orientation de la vitesse des écoulements souterrains. Pour ce faire un modèle numérique de puits a été construit avec la méthode des éléments finis afin d'effectuer des simulations numériques de la réponse thermique dans diverses conditions. À partir de ces simulations, il a été possible de démontrer le potentiel du concept de TRT et d'élaborer des méthodologies pour retrouver les propriétés désirées. Une méthode de résolution graphique est d'abord présentée. Dans un second temps, le formalisme des problèmes inverses est appliqué afin d'obtenir une deuxième méthode de mesure des paramètres du sol. Les résultats montrent que le TRT proposé permet de retrouver ces paramètres dans la plupart des scénarios envisagés.

Abstract

It is important to know the subsurface thermal conductivity and the groundwater flow parameters (i.e. its velocity and orientation) when sizing a geothermal borefield. This master's thesis presents a methodology and the conclusions of a numerical analysis of a novel thermal response test (TRT) concept for vertical geothermal heat exchangers. This configuration of TRT is able to measure both the hydraulic and the thermal properties of the ground. The main objective behind this work is to validate the concept and then to develop an efficient methodology to obtain from the thermal response of the TRT an estimation of the ground thermal conductivity along with the velocity and the orientation of groundwater flows. To achieve this, a numerical model of borehole was built using the finite element method. This model was then used to simulate the thermal response for various conditions. From these simulations, it has been possible to demonstrate the potential of the concept and to elaborate methodologies to find the desired properties. A graphical method is first presented. Following that, inverse problem techniques were applied to get a second measurement methodology. Results show that the suggested TRT is able to find the parameters in most of the cases.

Table des matières

Liste des tableaux

Liste des figures

Nomenclature

Lettres latines

A_0, A_1	Paramètres de corrélation
B	Distance entre deux puits, m
c_p	Capacité thermique, J/kg K
CF	Facteur de correction
f	Champ vectoriel
Fo	Nombre de Fourier
G	Fonction caractéristique
k	Conductivité thermique, W/mK
M	Nombre de capteurs de température
N	Nombre de puits
P	Pression, Pa
$\vec{p}$	Vecteur de paramètres inconnus
Pe	Nombre de Péclet
q	Taux de transfert de chaleur du puits, W
q'_0	Taux d'injection de chaleur de la source, W/m
R	Résistance thermique, mK/W
r	Coordonnée radiale, m
S	Norme des moindres carrées, $K^2 \times s$
t	Temps, s
T	Température, K, °C
u	Vitesse, m/s
x,y	Coordonnées cartésiennes, m
Y	Température mesurée, K, °C

Lettres grecques

α	Diffusivité thermique, m^2/s
κ	Perméabilité du sol, m^2
μ	Viscosité dynamique, $Pa \times s$

ρ	Densité, kg/m^3
η	Porosité du sol
χ	Ratio des capacités thermiques volumétriques
θ	Température relative $T-T_g$, K, °C
ϕ	Orientation de l'écoulement, °
τ	Temps d'un pulse, heure, mois, année
ω	Variable aléatoires
σ	Écart standard des erreurs de mesure, K, °C

Indices

avg	Moyen
b	Puits
c	Critique
calc	Calculée
cs	Capteur rapproché
D	Darcy
eff	Effective
ex	Exact
f	Fluide
fs	Capteur éloigné
g	Sol non-dérangé
H	Grande
h	Pulse par heure
Heat	Période de chauffage
i	Intérieur
L	Petite
M	Milieu
m	Pulse mensuel
Max	Maximum
o	Extérieur
p	Position de mesure

s	Solide
test	Test de réponse thermo-hydraulique
true	Vrai
U	Uniforme
y	Pulse annuel
0	Initial

Symboles

~	Non-dimensionnel
$\rightarrow$	Vecteur
$\bar{}$	Moyenné

Remerciements

Ce mémoire n'aurait jamais été possible sans l'aide de plusieurs personnes qui ont su contribuer de diverses manières. Je tiens à profiter de cet espace pour souligner leur contribution et les remercier.

Un incontournable est mon directeur de recherche, Louis Gosselin. Son apport a été essentiel à l'achèvement de cet ouvrage. Lorsque j'étais dans une impasse, il n'a jamais hésité à agir tel un guide pointant la bonne direction en plus de faire preuve de patience et de grande disponibilité. Louis est un passionné de la recherche, de la science et de la vie en général et je dois bien admettre qu'il m'a transmis cette passion. Je considère que c'est un privilège de pouvoir travailler avec un professeur aussi exceptionnel.

Mes remerciements suivant vont à tous mes collègues du *Laboratoire de Transfert Thermique et d'Énergétique* (LTTE). Durant ces années, j'étais entouré jour après jour d'une équipe dynamique formant une ambiance de travail fort agréable. Je tiens à remercier personnellement Maxime Tye-Gingras pour m'avoir enseigné les notions d'éléments finis nécessaires au démarrage de mon projet de recherche. Pour Ruijie Zhao, 谢谢 pour les divers trucs que tu m'as montrés lors de mon apprentissage du chinois! Merci à Alexandre, François, Jean-Michel, Jonathan, Maarten, Mathieu, Maxime, Noémie, Raphael, Richard, Ruijie et à tous les autres.

Mes derniers remerciements sont pour ma famille. D'abord, mes parents, Yves et Ginette, et ma sœur Marie-Josée, qui m'ont tous apporté un soutien financier, culinaire mais surtout moral pendant tout ce temps. Sans leur éducation et leur présence, je n'aurais sans doute jamais atteint ce point, autant d'un point de vue académique que personnel. Mes dernières lignes sont dédiées à ma marraine Sylvie et mon parrain Serge. Malgré les terribles défis qu'ils ont vécus, leur jovialité demeurerait toujours une source de motivation pour moi. À Sylvie, je dis : *Lâche pas la patate*!

Avant-Propos

Les deux articles présentés dans ce mémoire ont été coécrits par l'auteur de ce mémoire, Jean Rouleau, et son directeur de recherche, Louis Gosselin. Jean Rouleau, soit l'auteur principal de ces textes, a réalisé les recherches, l'élaboration du modèle numérique utilisé, les simulations numériques, l'analyse des résultats ainsi que la majorité de la rédaction des articles. Le second co-auteur, Louis Gosselin, fut le superviseur de ces travaux en guidant l'étudiant tout au long de ses recherches en plus d'aider à la rédaction et la correction des documents présentés. Le premier article a été co-écrit également par le professeur Jasmin Raymond, de l'INRS-ÉTÉ, qui a apporté son regard d'hydrogéologue lors de l'élaboration de l'article. Ces articles sont pour le moment soumis. Afin d'améliorer leur cohérence dans ce mémoire, quelques modifications mineures, telle que la numérotation des tableaux et figures et celle des références bibliographiques, ont étés apportées à leur version originale.

Chapitre 1 Introduction

1.1 Problématique

L'énergie géothermique représente l'énergie contenue sous forme de chaleur dans le sol. La présence de cette chaleur est due à la fois à la désintégration d'éléments radioactifs dans l'écorce terrestre et à la chaleur originale emprisonnée au cœur de la terre lors de sa formation. Une fois soutirée du sol par transferts thermiques, cette énergie peut servir divers secteurs : production d'électricité, chauffage et climatisation de bâtiments, chauffage de l'eau (autant pour les bains et piscines que pour la pisciculture), etc. Étant donné le faible gradient géothermique que l'on retrouve sur la plupart du territoire canadien, la géothermie au Canada a pour principale application de fournir de l'énergie à un système de pompe à chaleur, qui est autant en mesure de chauffer les bâtiments en hiver que de les climatiser en été. On dénote tout de même un certain potentiel de production d'électricité géothermique au Québec [1][2].

Bien que plus que négligeable avant les années 1990, le marché géothermique canadien est en impressionnante progression depuis les deux dernières décennies [3][4]. Le Canada ne fait pas bande à part puisqu'une tendance similaire est observable sur l'ensemble de la planète [5]. De par sa nature écologique, la géothermie cadre bien avec le développement durable et la protection de l'environnement. Toutefois, malgré cet intérêt croissant pour l'énergie du sol, cette technologie fait toujours face à des défis tels que la réduction des coûts de forage et le dimensionnement plus efficace des puits.

Un de ces défis est la difficulté de mesurer efficacement les propriétés du sol à une profondeur de l'ordre du 100 mètres. Pour concevoir un bon design d'un champ de puits géothermiques, il est essentiel de connaitre les propriétés du sol où on souhaite le construire. La conductivité thermique du sol est évaluée à partir d'une opération que l'on nomme test de réponse thermique (TRT). Cependant, bien que des études ont montré que la conductivité thermique est la propriété qui influence le plus la performance d'un échangeur géothermique, de plus en plus d'études indiquent également que les propriétés hydrauliques peuvent avoir une grande importance [6][7]. Par conséquent, de plus en plus de modèles de champs géothermiques requièrent la connaissance de la vitesse et de l'orientation de l'écoulement de l'eau contenu à l'intérieur des aquifères [8], puisque cet écoulement a un effet sur le transfert thermique se produisant entre les puits et le sol [9][10].

Les essais hydrogéologiques effectués [11][12] pour mesurer les écoulements souterrains sont coûteux en termes d'argent et de temps, et ne sont à toutes fins pratiques jamais utilisés pour des applications comme la géothermie. De leur côté, les tests de réponse thermique actuels ne considèrent pas ces écoulements souterrains; ils sont généralement basés sur une hypothèse d'échange de chaleur purement par conduction dans le sol [13]. Le fait d'ignorer le mouvement de l'eau peut induire, à moyen ou long terme, une erreur sur la performance réelle d'un champ géothermique par rapport à celle attendue. Il serait donc bénéfique de concevoir un test pouvant combiner l'aspect hydrogéologique à l'aspect thermique. L'étude présentée dans ce mémoire se consacre ainsi à l'établissement et la validation d'un nouveau concept de test de réponse thermique qui permettrait cette combinaison. Une telle implantation permettrait des économies d'argent, d'équipement, de main-d'œuvre et de temps.

1.2 Objectifs

1.2.1 Objectif principal

Ce projet de recherche a pour objectif principal de valider un nouveau concept de test de réponse thermo-hydraulique. Trois principaux points d'amélioration sont ainsi ciblés dans le projet : (1) Pouvoir estimer avec justesse la conductivité thermique du sol malgré l'influence des écoulements souterrains; (2) Mesurer les caractéristiques de l'écoulement hydrogéologique en même temps que les propriétés thermiques du sol et (3) Réduire les dépenses reliées au TRT.

1.2.2 Objectifs secondaires

- Concevoir un modèle numérique par éléments finis d'un puits vertical soumis à un écoulement hydrogéologique. Des simulations examinant le nouveau concept de TRT pourront y être produites.
- À partir des résultats obtenus par les simulations, bâtir une méthode d'analyse simple permettant de déterminer la conductivité thermique du sol en plus de la vitesse et de l'orientation de l'écoulement d'eau qu'il contient.

1.3 Méthode et présentation du document

Le montage suggéré de test de réponse thermique a dû être validé par une étude numérique, ce qui demande la modélisation numérique d'un domaine représentant un puits dans un sol où de l'eau s'écoule. La qualité première désirée pour ce modèle numérique était la rapidité à effectuer une simulation puisque ce modèle devait être utilisé à maintes reprises au cours de l'étude. Le modèle bâti est bidimensionnel pour cette raison. Le fait d'ignorer la dimension verticale requiert certaines hypothèses qui ont été jugées comme étant acceptables. Ce modèle a servi à la mise en place d'une méthode de résolution donnant les variables désirées selon la réponse thermique du montage. Deux méthodes distinctes offrent cette possibilité : une méthode graphique et une numérique, qui emploie des

principes de problème inverse de transfert de chaleur. Les deux ont été développées dans le cadre de ce travail.

Le mémoire a un format par articles; il est principalement constitué de deux articles scientifiques rédigés par l'auteur. Ces deux articles sont présentement soumis à des journaux scientifiques. Les sous-sections 1.3.1 et 1.3.2 introduisent les travaux contenus dans chacun de ces articles et expliquent en quoi ils ont mené à l'atteinte des objectifs du projet. La revue de littéraire nécessaire au projet est située dans l'introduction de ces deux articles.

1.3.1 Chapitre 2 – Nouveau concept de test de réponse combinée hydro-thermique pour échangeurs de chaleur géothermique

Cette section est l'intégrale du premier article rédigé par l'auteur de ce mémoire qui introduit les lecteurs au nouveau concept suggéré de TRT. L'article est présentement soumis au journal Geothermics. Dans un premier temps, une description sommaire du concept est effectuée. Puis, la section suivante de l'article explique le système d'équations mathématiques qui régit le problème étudié avant de présenter le modèle numérique qui a été bâti pour résoudre ce système avec un logiciel d'éléments finis [14]. La section 2.4 montre l'impact des écoulements souterrains sur la réponse thermique du montage; les résultats obtenus à cette section permettent de développer une démarche graphique d'estimation des paramètres désirés à la section suivante.

Cet article permet de répondre aux objectifs de la section 1.2.2, c'est-à-dire qu'il offre, à partir d'un modèle numérique, une manière d'estimer les trois paramètres désirés. À la suite de certains essais de cette méthode, des recommandations sont offertes par rapport aux trois principales variables du test qui sont choisies lors d'un TRT, soit le taux d'injection de chaleur employé pour la source, le rayon du puits où le test est exécuté et la durée de la période de chauffage. Avec cet article, un ingénieur possède tous les outils nécessaires pour reproduire sur le terrain le nouveau test de réponse thermique suggéré.

1.3.2 Chapitre 3 – Emploi de concepts de résolution de problème de transfert thermique inverse pour la mesure des propriétés hydro-thermiques du sol

Ce chapitre présente une nouvelle configuration du TRT, qui devrait faciliter la mise en place sur le terrain du montage requis. Toutefois, ce changement élimine l'aspect symétrique du problème étudié; la démarche graphique présentée lors du premier article ne peut donc pas être employée pour cette disposition. Il y a ainsi eu un besoin d'établir une méthode différente d'estimation des paramètres désirés. Celle-ci est plutôt d'ordre numérique avec l'emploi d'outils de résolution de problèmes inverses. L'article formant ce chapitre du mémoire présente la capacité de la méthode de résolution de problèmes inverses à mesurer les propriétés du sol en plus d'offrir une idée sommaire de l'impact que les incertitudes de mesure des capteurs de température ont sur la qualité des estimations.

Ainsi, le second article contribue également à l'atteinte des sous-objectifs établis puisqu'il offre une alternative à la démarche présentée lors du premier article. L'énorme avantage que possède cette autre méthode est sa polyvalence; elle peut être adaptée à toutes les situations possibles. Le modèle numérique préétabli a dû être adapté et il a fallu coupler le programme d'éléments finis employés avec le logiciel *Matlab* pouvant minimiser une fonction objective. Cette opération a demandé de construire un script d'optimisation.

Chapitre 2 Article de revue

Titre

NEW CONCEPT OF COMBINED HYDRO-THERMAL RESPONSE TESTS (H/TRTS) FOR GROUND HEAT EXCHANGERS

Co-auteurs

Jean Rouleau, Louis Gosselin, Jasmin Raymond

Journal

Geothermics – Article soumis en date du 14 août 2015

Résumé

Les tests de réponse thermique actuels, qui sont utilisés afin d'évaluer la conductivité thermique d'un champ géothermique, ne sont pas conçu pour considérer les écoulements d'eau souterrains. Pour mesurer les paramètres de ces écoulements, un nouveau concept a été développé. Des câbles de chauffage sont installés dans un puits qui se trouve en contact direct avec la formation souterraine. Ces câbles sont entourés de trois capteurs de température placés de manière stratégique au périmètre du puits. L'étude de l'évolution de la température pour chaque capteur durant une période chauffage et une période de restitution thermique permet de déterminer la conductivité thermique du sol, en plus la vitesse et de l'orientation de l'écoulement d'eau qu'il contient. Des simulations numériques ont été utilisées pour valider le potentiel de ce concept et établir ses limites.

Abstract

Current thermal response tests, used to estimate the subsurface thermal conductivity in the geothermal sector, are not designed to take into account groundwater flows. To measure the flow parameters, a new concept has been developed. Heating cables are installed within a borehole in contact to the formation, with three temperature probes strategically located at the edge of the borehole. Study of the evolution of temperature for each probe during both a heat injection phase and a recovery period allows determining ground thermal conductivity, groundwater flow velocity and orientation. Numerical simulations have been used to validate the proposed concept and establish its limits.

2.1 Introduction

The increasing demand for clean energy and the growing concerns over global warming and emissions of CO_2 have led to a regain of interest for green energies. Over the last decades, the use of ground-coupled heat pump (GCHP) systems has developed fast. The number of units installed per year in Canada has grown by a factor close to 1 000% between 2000 and 2010 [15]. GCHP systems transfer heat to the ground (or from the ground) for space heating or cooling in residential and commercial buildings. For a good sizing of borehole heat exchangers (BHEs), engineers need to properly estimate the thermal properties of the ground. Thermal conductivity is an essential parameter in order to characterize the heat transfer between a ground heat exchanger and the surrounding subsurface. Thermal response tests (TRTs) are used for in situ measurement of the subsurface thermal properties. In a typical TRT, the evolution of the temperature of the water circulating in the BHE is measured at the inlet and outlet of the BHE. Then, using Kelvin's line source theory, which is based on Fourier's law of conduction, or based on other models to represent heat transfer around the borehole, it is possible to deduce the ground thermal properties [16][17][18][19][20]. Kelvin's line source model assumes an infinite, homogenous and isotropic ground in which heat transport in the ground is completely driven by conduction [13].

Unfortunately, the assumptions on which this model relies can turn out to be false. One of the most significant limitations is the lack of consideration of convective heat transfer in the ground. Geothermal borefields can be installed in aquifers. If the geological materials is sufficiently permeable or submitted to a strong hydraulic gradient, groundwater will move through the ground pores or fractures, which affects heat transfer around BHEs [21][22][23]. Since the line source model neglects groundwater flows, it has been shown that TRTs in such cases can provide wrong estimates of the subsurface thermal conductivity [19][24][25][26], and most importantly, oversizing of the BHEs. Advection enhances heat transfer between the BHE and the subsurface, which means that shorter BHEs than in the absence of groundwater flow can be installed to satisfy the same load. Analytical [27][28] and numerical [29][30][31][32] models were established to simulate heat transfer around a BHE with groundwater flow. Nevertheless, current TRTs do not

provide information on the hydrogeological information required to size the borefield, namely groundwater velocity and direction.

Accounting for groundwater flows is primordial when designing GCHP systems [6]. In recent works, it has been demonstrated that neglecting groundwater flow in design procedure can induce an overdesign of the borefield length that can go up to 68% [8]. Engineers not only need to consider groundwater flowrate, but the direction of the flow is also an important parameter [7]. These parameters have to be known when applying adequate models for the design of geothermal borefield. Determining such parameters requires hydrogeological tests which might be prohibitive in terms of time and cost when designing and installing a GCHP system. Therefore, there is a need to develop a combined hydrogeological and thermal test to acquire the required estimates of ground properties in the design process.

Another possible point of improvement to current TRTs is to obtain a subsurface thermal conductivity profile instead of an average value. Other alternative tests have been proposed to obtain a profile of the ground properties, with the use of optical fibers [33][34][35] or thermostratigraphy [36]. However, these methods are either highly expensive or require the knowledge of additional data such as the local Earth natural heat flow.

In this paper, we address some of the shortcomings mentioned above by developing a configuration of combined hydro-thermal response tests (H/TRT). This H/TRT is inspired by the work of Raymond [37][38], in which a heating cable is placed in a borehole to inject heat in the subsurface during the TRT. Theoretically, with multiple temperature probes positioned in a horizontal plane around the cable, it is possible to observe the strength and direction of groundwater flow. Using heating cable sections to directly generate heat in the borehole requires less power than conventional TRT and less equipment. It is also possible to obtain a vertical profile of the ground thermal conductivity if the test is simultaneously accomplished at various depths. Continuous heating cables can also be used, but require high tension to provide enough heat.

The objective behind this paper is to use numerical simulations to validate the potential of the concept before performing field experiments. The first part of the paper details the concept and the numerical model that was built to simulate its performance in

various possible geological cases. Results are then shown in the following sections. From these results, a methodology is proposed to accurately estimate the subsurface thermal conductivity and groundwater flow parameters.

2.2 Description of the concept

Based on the work of Raymond et al. [37], the proposed concept of H/TRT uses a heating cable placed in a borehole to inject heat in the subsurface. This strategy to inject heat in the borehole has already been numerically validated for the measurement of thermal conductivity [38] and yielded promising results based on in situ testing in U-tube ground heat exchangers [39]. In the present paper, however, the heating cable is installed directly in the "empty" borehole (not in the U-tube) that is in contact with the formation. Moreover, groundwater flows have not been considered thus far in that type of tests, hence the need for an adaptation to account for them. In order to do so, it is proposed to use three temperature sensors (instead of one) to measure the evolution of the temperature in the borehole during the heat injection from the source. These probes are distributed uniformly on the edge of the well (i.e., at an interval of 120 degrees). The cable is positioned at the center of the hole. Since the heat plume generated by the source is deformed in the direction of the groundwater flow, each sensor will monitor different temperature evolutions. Therefore, by comparing every sensor measurement, one could potentially estimate the ground thermal conductivity, along with the groundwater flow parameters (i.e., velocity and orientation). The test is performed in a borehole before it is filled with grout. The proposed setup is sketched in Fig. 2.1.

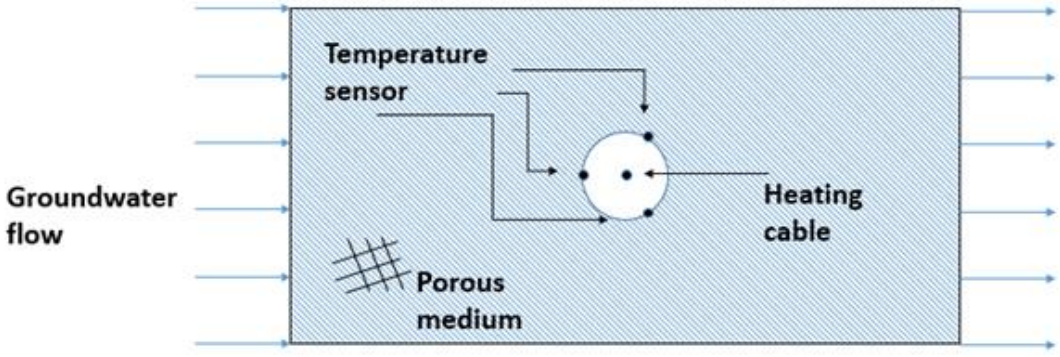

Figure 2.1 - Schematic representation of the proposed H/TRT setup with groundwater flow.

The idea behind the H/TRT is similar to that employed by hydrogeologists measuring the hydraulic head at three different wells to determine groundwater flow velocity and direction [11]. The differences are that temperature is the variable measured instead of the hydraulic head, and the test is performed in a single well. In order to constrain the measurement of groundwater flow parameters within a single well, hydrogeologists can also employ a heat-pulse groundwater flow meter, which uses a similar approach to the proposed H/TRT, but cannot provide estimation of the ground thermal conductivity [12]. Lee and Lam proposed a test where they monitored three concurrent standard TRTs in three adjacent boreholes [40]. Other ways of obtaining hydraulic characterization from temperature data have been suggested in the past [41][42]. Simultaneous TRTs and well tests executed in a single borehole greatly reduce both the duration of the test and the equipment needed.

In the present H/TRT, it is proposed to record the probes temperature for a certain period of heating (e.g., three days), followed by a recovery period (no heating) of equivalent duration. The exact position of the sensors and of the heat source might not be precisely known, which can lead to uncertainties on the measured ground properties. It was found that the recovery period can help to reduce these potential errors since the temperature field tends to become more uniform during recovery [43].

2.3 Mathematical and numerical models

Numerical simulations have been performed in order to establish the potential of the H/TRT approach presented in Section 2. Numerical models are fairly easy-to-use and offer the possibility of measuring precisely the individual impacts of various parameters, such as the subsurface thermal conductivity or the groundwater flow rate. Heat transfer in the presence of groundwater flow is a complex process that combines both conduction and advection. The finite element method (FE) has been used to simulate heat transfer and groundwater flow.

Table 2.1 Typical groundwater Darcy velocity in various geological materials [44]**.**

Aquifer materials	Hydraulic conductivity [m/s]	Darcy velocity* U_D [m/s]	Thermal conductivity k_{avg} [W/mK]	Volumetric heat capacity ρc_p [10 MJ/m^{3}K]
Gravel	10^{-4}-10^{-2}	10^{-7}-10^{-5}	1.8	2.4
Coarse sand	10^{-3}	10^{-6}	1.7-5.0	2.2-2.9
Medium sand	10^{-4}	10^{-7}	1.7-5.0	2.2-2.9
Fine sand	10^{-6}-10^{-5}	10^{-9}-10^{-8}	1.7-5.0	2.2-2.9
Silt	10^{-7}	10^{-10}	0.9-2.3	1.6-3.4
Clay	10^{-10}-10^{-9}	10^{-13}-10^{-12}	1.2-1.5	2.3

* Assuming hydraulic gradient of 0.001 m/m

Readers are referred again to Fig. 2.1 to see the numerical domain. It consists of a borehole of radius r_b embedded in a saturated porous medium. Dry ground is seen as the matrix of the porous medium and its pores are filled with water (saturated ground). Table 2.1 offers typical values of thermal and hydraulic properties for different geological materials, assuming a hydraulic gradient of 0.001 m/m [44]. While properties for dry ground were consistently modified between each simulation, properties of water used by the model remained fixed and are given in Table 2.2. Preliminary simulations showed that groundwater flow had a negligible impact on TRT for flows with Darcy velocity inferior to 10^{-8} m/s, hence properties of silt and clay were not considered in this study. Materials are assumed to be isotropic. Dimensions of the numerical domain were normalized by the borehole radius – its length was 85 times longer than the radius of the borehole while its height was 42.5 times larger. The borehole radius length varied between $r_b = 0.05\,\mathrm{m}$ and $r_b = 0.1\,\mathrm{m}$ depending on the simulation case.

Table 2.2 Properties of water for the numerical model [45].

Properties	Value
ρ_w [kg/m^3]	999
μ_w [kg/ms]	$1.08 \cdot 10^{-3}$
k_w [W/mK]	0.598
$c_{p,w}$ [J/kgK]	4 184

2.3.1 Governing equations

The physical laws governing the problem are the conservation of mass, momentum and energy. In order to limit the computational time, the domain was approximated as two-dimensional. The first two laws are considered in the Navier-Stokes equation, modified to take into account the porous medium. Since the velocity and pressure fields were assumed not to change with time, a steady-state version of the equations was considered:

$$\rho \nabla \cdot \vec{u} = 0 \tag{2.1}$$

$$\frac{\rho}{\eta}\left((\vec{u}\cdot\nabla)\frac{\vec{u}}{\eta} \right) = \nabla \cdot \left(-P + \frac{\mu}{\eta}\left(\nabla\vec{u} + (\nabla\vec{u})^{T} \right) - \frac{2\mu}{3\eta}(\nabla\cdot\vec{u}) \right) - \frac{\mu}{\kappa}\vec{u} \tag{2.2}$$

This formulation has the advantage that it is valid both in the ground (porous media with a finite value for the permeability) and in the well itself (where the last term of Eq. (2.2) vanishes). Therefore, the same set of equations can be solved in the entire domain. Far from the borehole, an easy way to approximate the average groundwater flow velocity is to use the Darcy's velocity:

$$u_{r\to\infty} \equiv u_D = -\frac{\kappa_g}{\mu}\frac{\partial P}{\partial x} \tag{2.3}$$

The conservation of energy equation must include both conduction and advection. In a porous medium, it reads as

$$(\rho c_p)_f \left(\chi \frac{\partial \theta}{\partial t} + \vec{u}\cdot\nabla\theta \right) = \nabla \cdot (k_{avg}\nabla\theta) \tag{2.4}$$

where:

$$\theta = T - T_g \quad , \quad \chi = \frac{\eta(\rho c_p)_f + (1-\eta)(\rho c_p)_s}{(\rho c_p)_f} \tag{2.5}$$

Note that the index "avg" for k is to indicate the average ground thermal conductivity around the borehole. The values of thermal conductivity and thermal diffusivity depend on the porosity of the ground matrix:

$$k_{avg} = \eta k_f + (1-\eta)k_s \quad , \quad \alpha_{avg} \equiv \frac{k_{avg}}{(\rho c_p)_f} \tag{2.6}$$

Other ways to calculate the average conductivity exist. However, it should be noted that what is important for the mathematical modelling of the problem is the thermal conductivity of the porous medium itself, and not the decomposition between the matrix

and its pores. Therefore, for simplicity, the arithmetic mean was used to compute the average value of thermal conductivity even though other models are available. Again, the advantage of Eq. (2.4) is that it can be used in the entire domain. In the well, there is only water and no dry ground, meaning that for that part of the domain, conservation of energy is represented by:

$$\left(\rho c_p\right)_f\left(\frac{\partial\theta}{\partial t}+\vec{u}\cdot\nabla\theta\right)=\nabla\cdot\left(k_f\nabla\theta\right) \tag{2.7}$$

In order to limit the number of variables, the problem was solved with dimensionless variables:

$$\begin{aligned}&\tilde{x},\tilde{y}\equiv\frac{x,y}{r_b},\quad \tilde{\vec{u}}\equiv\frac{\vec{u}r_b}{\alpha_{avg}},\mathrm{Pe}\equiv\frac{u_D r_b}{\alpha_{avg}},\quad \mathrm{Fo}\equiv\frac{t\alpha_{avg}}{r_b^2},\\&\tilde{\theta}\equiv\frac{2\pi k_{avg}\theta}{q_0'},\quad \tilde{k}\equiv\frac{k_{avg}}{k_f}\quad\text{and}\quad \tilde{P}\equiv\frac{P\kappa_g}{\mu\alpha_f}\end{aligned} \tag{2.8}$$

Here, q_0' presents the heat injection rate of the source during the heating process. The ground effective volumetric heat capacity has to be known for the calculations of Fo and Pe. According to [46], the volumetric heat capacity can be estimated solely based on the identification of the host rock where the borehole is drilled with an uncertainty of ±15%. Based on the data from Tables 2.1 and 2.2, ranges employed for each dimensionless scales can be seen in Table 2.3. The velocity vector can be expressed as a product between the Peclet number Pe and a dimensionless vector function:

$$\tilde{\vec{u}}\left(\tilde{x},\tilde{y}\right)=\mathrm{Pe}\cdot\vec{f}\left(\tilde{x},\tilde{y}\right) \tag{2.9}$$

Using these scales, Eqs. (2.4) and (2.7) can be reduced to:

$$\chi\frac{\partial\tilde{\theta}}{\partial\mathrm{Fo}}+\mathrm{Pe}\cdot\vec{f}\left(\tilde{x},\tilde{y}\right)\cdot\tilde{\nabla}\tilde{\theta}=\tilde{k}\tilde{\nabla}\cdot\tilde{\nabla}\tilde{\theta} \tag{2.10}$$

$$\frac{\partial\tilde{\theta}}{\partial\mathrm{Fo}}+\mathrm{Pe}\cdot\vec{f}\left(\tilde{x},\tilde{y}\right)\cdot\tilde{\nabla}\tilde{\theta}=\tilde{\nabla}\cdot\tilde{\nabla}\tilde{\theta} \tag{2.11}$$

The entire domain is initially at $\tilde{\theta}=0$. Far from the borehole, the temperature of the boundaries is fixed at the initial value. A pressure gradient is imposed to generate the groundwater flow. While the value of $\tilde{P}$ at the left boundary varies according to the desired groundwater velocity, the dimensionless pressure of the right side remains $\tilde{P}=0$

for all simulations. This means that groundwater flows in the numerical domain from left to right.

Table 2.3 Simulated range for all variables.

Variable	Values tested
Pe	10^{-3} to 10^{-1}
Fo	0 to 1 000
$\tilde{k}$	2 to 8

In developing this model, the following assumptions were made:

(i) Local thermal equilibrium is assumed, i.e. water and ground temperatures are the same locally;

(ii) Groundwater flow is assumed to be unidirectional and parallel to the ground surface. Furthermore, groundwater flow is supposed to be present everywhere in the aquifer and to be stationary over the duration of the test;

(iii) The heat transfer is also assumed to be parallel to the ground surface. This assumption is fairly good considering the short periods of time over which tests are performed [47].

(iv) All properties are assumed to be uniform and non-affected by temperature;

(v) Dispersivity is not considered explicitly in the model. Although some models account for it [26][44][48], few data is available for quantifying thermal dispersion of typical groundwater flows.

(vi) Natural convection inside the well is neglected. It has been proved that for TRT using heating cable, natural convection can be greatly limited with perforated disks positioned at strategic vertical positions to cut off possible circulating loops [38]. Tests based on the heat-pulse groundwater flow meter usually limits natural convection with the use of packers. Executing the test with continuous heat cable also minimize natural convection if the setup is properly done [49]. Under certain

conditions (particularly when the Darcy flow is small), natural convection could have an impact – a 3D model could be helpful to assess this impact.

2.3.2 Numerical model

To solve numerically the above-mentioned differential equations within the domain, a commercial finite element software was used [14]. The mesh generated has unstructured triangular elements that are concentrated around the borehole, where high temperature gradients are expected due to the presence of the heat source. Considering the symmetry of the domain, only half of the domain needs to be simulated. An infinite element zone that was 8.5 time longer than the radius of the borehole was added to the model boundary. It was verified that the domain dimensions had no effect on the simulation results, i.e. that when a larger domain is used, the results stay the same. Time stepping needed to solve the energy equation is automatically chosen by the software during simulation, adjusted with a relative tolerance of 10^{-3}.

To ensure the correctness of the results, mesh convergence was verified. The mesh independence was considered to be reached when doubling the number of elements in the domain yielded a relative discrepancy of less than 1% on the average probes temperature for every time-step in the considered range. The mesh independence study was performed with groundwater flowing far from the borehole at a Peclet number of Pe = 0 and Pe = 0.1. For typical values of $\alpha_{eff} = 10^{-6} m^2/s$ and $r_b = 0.075 m$, a Peclet number of 0.1 translates to a Darcy velocity of $u_D = 1.33 \cdot 10^{-6} m/s$. These correspond to extreme parameter values, hence the chosen mesh can be applied to every simulation cases if it works for these. The final mesh that was used for simulations contained 7,944 elements and is shown in Fig. 2.2.

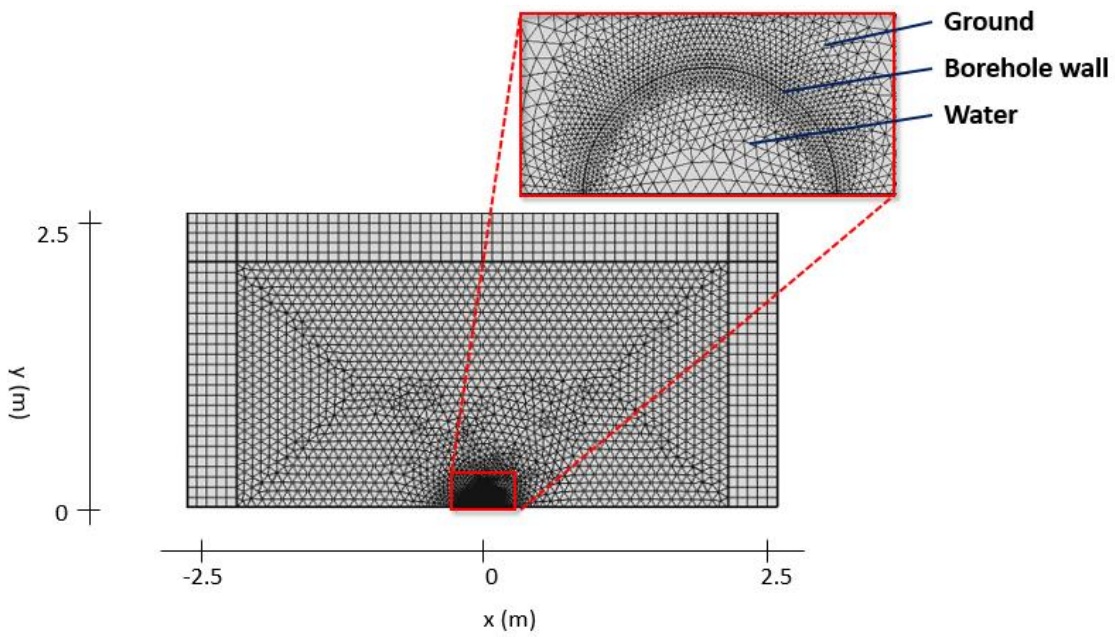

Figure 2.2 – Mesh of the numerical model used for simulation of the proposed H/TRT setup with groundwater flow.

2.4 Influence of groundwater flow during H/TRT

In order to assess the heat transfer mechanisms during the H/TRT proposed in this paper, numerical simulations were carried out. Simulations were performed to evaluate the impacts of advection on the thermal response of the system. Simulations did not account for variations of χ as there is a limited range of possible values for this parameter in typical permeable geological materials. A value of $\chi = 0.6$ was considered for all simulations.

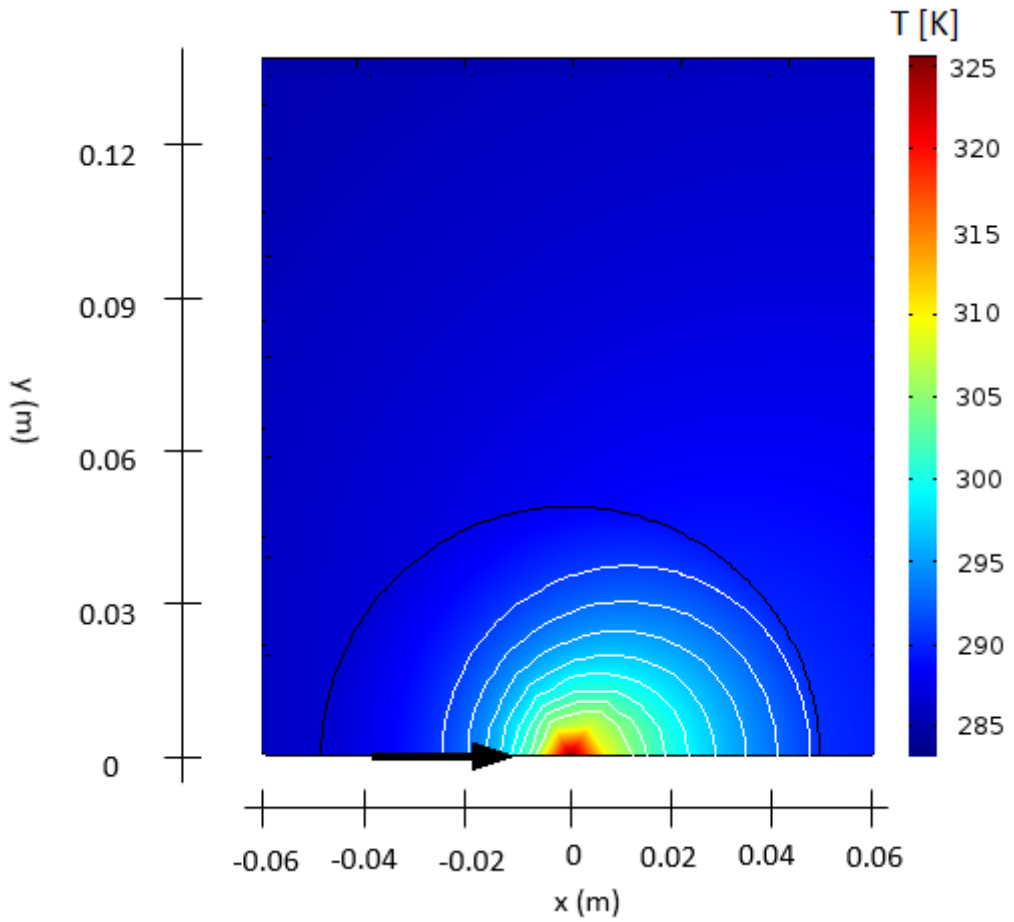

Figure 2.3 - Example of simulated temperature profile in and around the borehole after a day of heating (isotherms with a 2 K increment are shown).

To observe the impact of groundwater flows during the suggested TRT concept, the thermal response created by the heat source was simulated for multiple values of the Peclet number (Pe). Although the influence of advection on the transient evolution of a borehole average temperature has been investigated before, the distribution of temperature produced within the borehole by groundwater flows has received considerably less attention. Fig. 2.3 offers a view of the distribution of temperature in the borehole for a flow of $\mathrm{Pe} = 0.1$, after a day of heating. A ratio of thermal conductivities of $\tilde{k} = 4$ and a power input of 40 W/m for the heat source were used. The center of the borehole, where the cable is positioned, is clearly the warmest area of the domain. The white lines, which represent isothermal lines, are not axisymmetric around the heat source – they are pushed towards the flow orientation, which is represented by the arrow in Fig. 2.3. Therefore, temperature at different positions

along the borehole perimeter should read different temperatures. This is confirmed by Fig. 2.4, which presents the thermal response at seven positions along the borehole perimeter at an increment of 30 degrees for four distinct values of Pe. A dimensionless duration of $\mathrm{Fo} = 50$ was used for the heating period. The influence of groundwater flow can easily be seen when comparing the curves of Fig. 2.4. Because the heat plume generated by the source stretches in the direction of the flow, sensors that are aligned with the groundwater flow read higher temperatures than the ones that are opposite to the flow, thus creating a difference of temperatures between the sensors. This difference of temperatures widens as Pe increases. In the case of $\mathrm{Pe} = 0.1$, the gap of temperature between sensors is higher than 1°C during most of the heating period, making it possible to notice the influence of subsurface flow. Again, such a Peclet number can easily be reached with a Darcy velocity of $u_D \sim 10^{-6}\,\mathrm{m/s}$. On the other hand, the curves for $\mathrm{Pe} = 0.01$ are similar to the thermal response of the purely conductive case. As a result, with a heat injection rate of 40 W/m, it appears that the setup cannot properly detect advection at such a low Peclet number value.

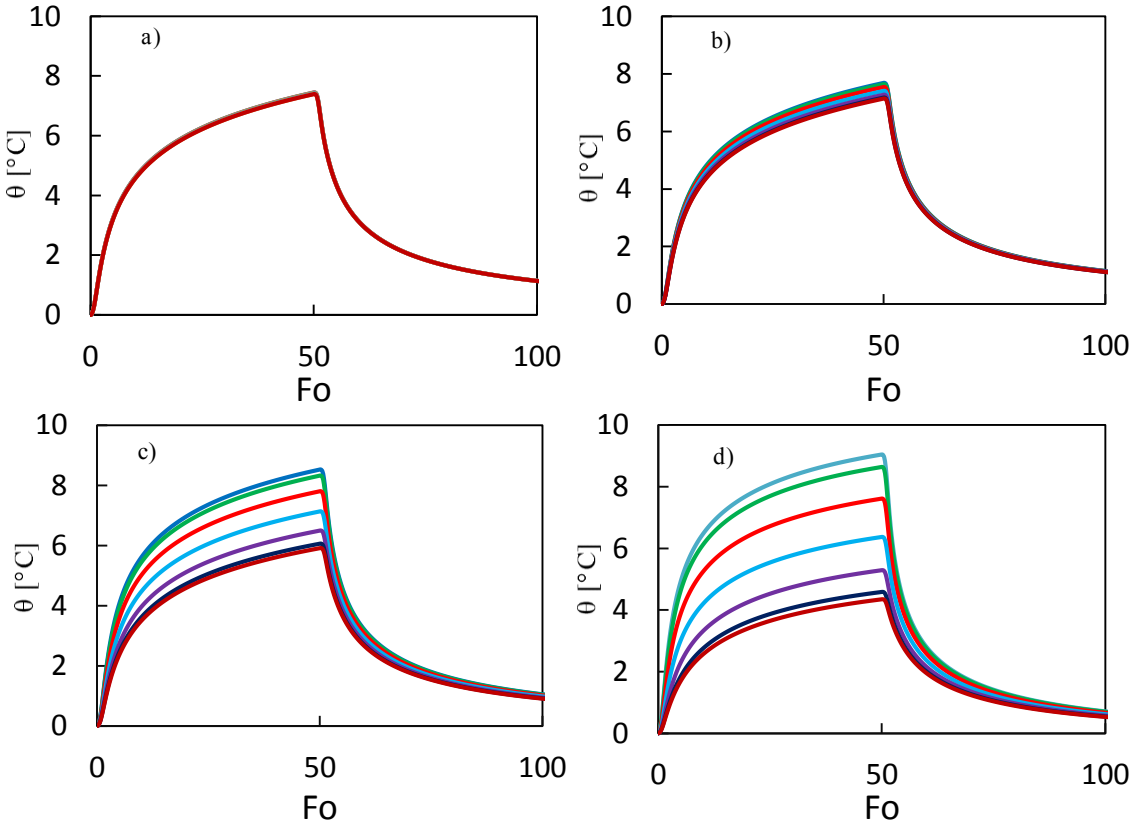

Figure 2.4 - Example of temperature evolution measured by sensors for a) Pe = 0.001 b) Pe = 0.01 c) Pe = 0.05 and d) Pe = 0.1. Each color represents a different sensor.

As expected, for all Pe values, during the recovery stage, differences of temperature quickly vanish as temperature in the borehole becomes uniform in a short period of time. A uniform temperature in the borehole can be beneficial because of the evaluation the thermal conductivity becomes less sensitive to the exact position of the cable and sensors within the borehole. Additionally, since the borehole itself is included in the radius of influence of the H/TRT around the heating cable during the injection phase, and since the borehole is filled only by water (which has a low thermal conductivity), a thermal conductivity determined during the heating phase would tend to underestimate the ground thermal conductivity. During the recovery phase, the uniform temperature in the water fixes this issue as there is no heat transfer in the borehole itself as Fo increases.

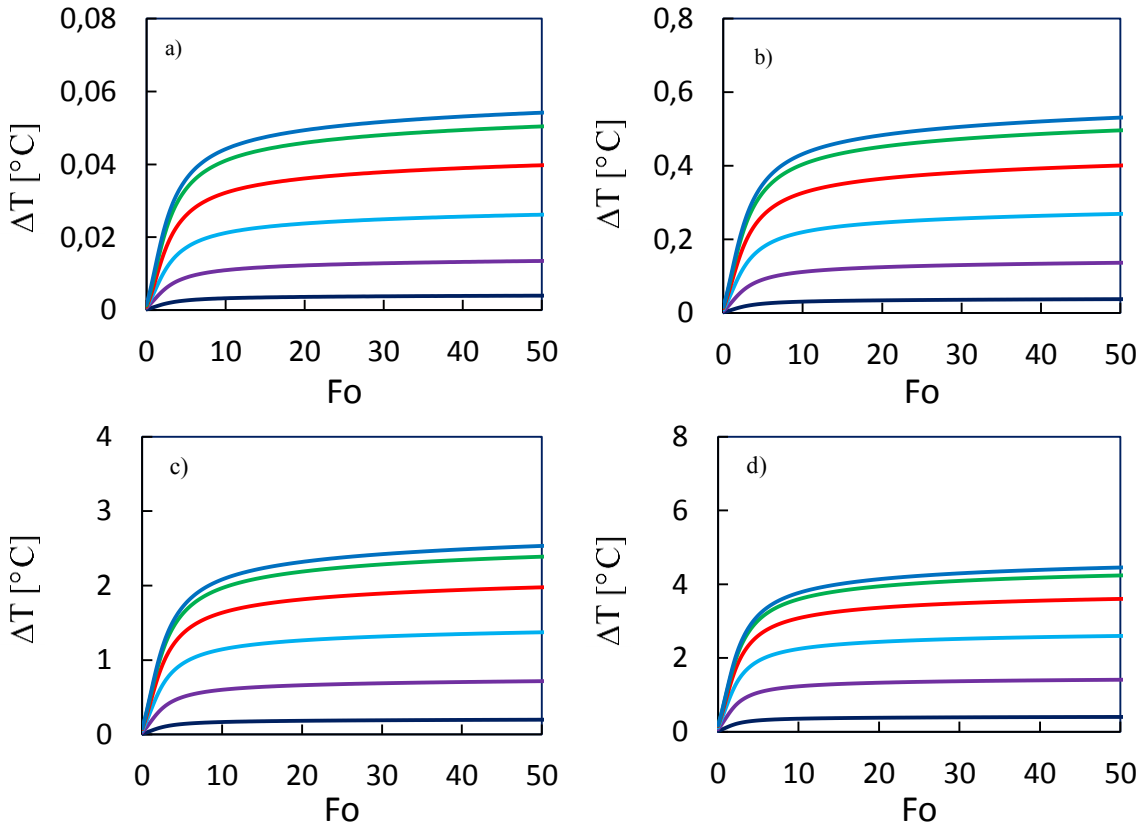

Figure 2.5 - Example of the evolution of the differences of temperature between sensors for a) Pe = 0.001 b) Pe = 0.01 c) Pe = 0.05 and d) Pe = 0.1. Each color represents the difference of temperature between the probe installed at the warmest position and a different probe.

Concerning the differences of temperature between the sensors, it was found that they build up quickly in the early stage of the heating period $(\mathrm{Fo} < 10)$. Rapidly, despite of the fact that no steady-state condition is reached, the differences of temperature follow a nearly-constant evolution and progress slowly. In other words, the temperature increases at the same pace for all sensors. This pattern was the same for all Pe as presented in Fig. 2.5. It shows the difference of temperature between the sensor reading the highest temperature and the six other probes.

2.5 Proposed methodology for H/TRT analysis

Section 4 has shown the impact of groundwater flow during the thermal response of the H/TRT setup. The object of the H/TRT is to determine three main parameters: the ground effective thermal conductivity, the groundwater flow velocity and orientation. By evaluating properly the thermal response, it could be possible to isolate the impact of each of these parameters and then to estimate their values. Here, a method to do so will be developed.

2.5.1 Evaluation of the groundwater flow orientation

Since the determination of the flow orientation does not require a particular knowledge of ground properties and is helpful for the estimation of Pe, it is suggested to start the analysis there. A methodology similar to that used in hydrogeology is proposed to find the orientation of the groundwater flow from an H/TRT. In hydrogeology, the path of a subsurface flow is found by locating the equipotential lines. Equipotential lines are the lines where the hydraulic head remains constant. Since the motion of water is strictly driven by the hydraulic gradient, the flow has to be perpendicular to such lines in an isotropic medium. Therefore, if the hydraulic head is known at three different horizontal positions, it is possible to interpolate the direction of equipotential lines and thus to know the orientation of the flow. Although this method is relatively precise, it has the disadvantage that it requires three boreholes to be drilled.

Here, instead of the hydraulic head, it is the temperature that is measured at three distinct positions within a single borehole. This means that the suggested setup cannot

directly determine equipotential lines, but it allows users to identify the isothermal lines, hence a similar approach can be used. The direction of the flow was estimated to be the parallel to the gradient of the plane formed by the temperature values measured at the three sensor points. Since advection carries the heat generated by the source in the flow direction, the heat plume described by isothermal lines should be parallel to the motion of groundwater (Fig. 2.3). Simulations were performed to verify this hypothesis and assess the measurement error on the flow direction adopting this method, for different values of Pe. Table 2.4 shows the outcome of this investigation, which was done with $\tilde{k} = 4$ and a heat rate of 40 W/m. It shows the flow direction determined from the isotherms compared to the actual orientations, for three cases. This study was repeated for different ratios of conductivities, and the results were similar as will be shown later. To correctly represent real thermal sensors, temperatures calculated with the numerical model were rounded to the nearest tenth. In most cases when $\mathrm{Pe} < 0.005$, the setup is not sensitive to groundwater flow and therefore the orientation measurement was impracticable. However, the impact of the groundwater flow on the heat transfer between the borehole and the ground is negligible for these values of Darcy velocity, and therefore, for the sizing of boreholes, this data is actually not that useful. In other words, the knowledge of the flow orientation is not vital at low Pe numbers. When Pe is higher, the error on the measurement was found to be inferior to 15°. The method was more effective for a flow of $\mathrm{Pe} = 0.05$ than a flow of $\mathrm{Pe} = 0.1$. This is caused by the fact that the heat plume generated by the source becomes narrower for great velocities. Sensors located outside of the plume are not affected by the heat source which can lead to wrong estimate of the orientation. The temperature measurements were taken at the end of the heating stage in this study.

Table 2.4 Direction calculated after a day of heating for different groundwater velocities.

Peclet number Pe [-]	**Calculated direction** $(\phi_{true} = 70°)$ **[°]**	**Calculated direction** $(\phi_{true} = 147°)$ **[°]**	**Calculated direction** $(\phi_{true} = 271°)$ **[°]**
0.005	60.0	138.2	270.0
0.01	74.5	145.2	263.1
0.05	72.5	143.1	268.4
0.1	76.0	140.8	265.4

2.5.2 Evaluation of groundwater flow velocity

Referring back to Figs. 2.4 and 2.5, it can be seen that the main effect of the groundwater flow velocity is to increase the differences of temperature measured by the sensors on the periphery of the borehole. This increase happens during the early stage of the heating period and the differences of temperature are nearly constant later. Accordingly, the maximal difference of temperature on the borehole perimeter ΔT_{max} appears to be essentially proportional to the flow velocity. As shown in Fig. 2.6, ΔT_{max} is defined as the difference of temperature between two sensors on the borehole perimeter that would be aligned in the direction of the flow, i.e. one upstream and one downstream. In practice, if the flow orientation ϕ is known and a gap of temperatures is sensed between each sensor, a trigonometric calculation gives a good approximation of ΔT_{max} via extrapolation:

$$
\begin{aligned}
T_{max} &= T_H + (T_H - T_L)\frac{1-\cos\beta}{\cos\beta - \cos(\beta+120°)} \\
T_{min} &= T_L - (T_H - T_L)\frac{1-\cos(\beta+120°)}{\cos\beta - \cos(\beta+120°)} \\
\Delta T_{max} &= T_{max} - T_{min}
\end{aligned}
\qquad (2.12)
$$

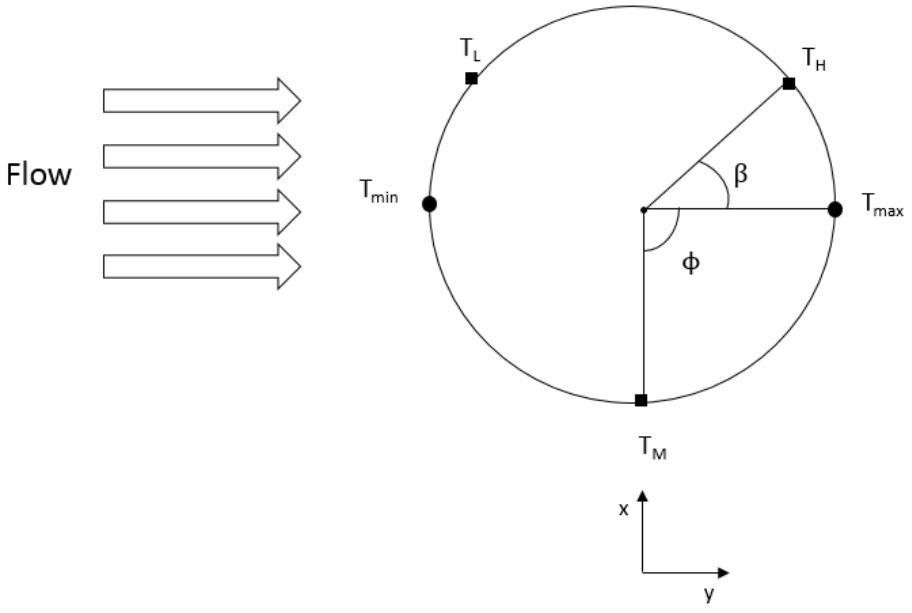

Figure 2.6 - Schematic view of the borehole during the test to illustrate the definition of ΔT_{max} .

Equations (2.12) assumes that the temperature field in the borehole can be approximated by a plane. Note that the angle β used in Eq. (2.12) is not necessary equal to ϕ - ϕ is the angle between the flow orientation and a reference x-axis and β is the angle between the flow and the sensor with the highest temperature value, which is not necessarily along the reference axis. To reduce the number of variables, ΔT_{max} has been translated into a dimensionless parameter:

$$\Delta\tilde{T}_{max} = \frac{k_f \Delta T_{max}}{q'_0} \tag{2.13}$$

Equations (2.12) shows that the extrapolation of $\Delta\tilde{T}_{max}$ depends on the value of the flow orientation taken into account by the angle β. As a result, the accuracy of the extrapolation is influenced by the evaluation of β. Table 2.5 shows how dependent the determination of $\Delta\tilde{T}_{max}$ is to the flow orientation. For the sake of illustration, the test was done with $\tilde{k} = 4$ and Pe = 0.05 at a flow orientation of $\phi = 30°$. $\Delta\tilde{T}_{max}$ was calculated at Fo = 50. Other sets of parameters were also considered with similar results. The table shows that Eqs. (2.12) provide a satisfying estimate of $\Delta\tilde{T}_{max}$ even when β is not precisely known. When the error on the flow orientation evaluation is lower than ±20°, extrapolating $\Delta\tilde{T}_{max}$ with Eqs. (2.12) leads to accurate results (errors smaller than 10%).

Table 2.5 Error on the extrapolation of the maximal difference of temperature calculated with Eqs. (2.12) according to the accuracy of the flow orientation measurement ($\Delta\tilde{T}_{max,true} = 3.78 \times 10^{-2}$).

Error on β [°]	**$\Delta\tilde{T}_{max,calc}$ [10^{-2}]**	**Relative error on $\Delta\tilde{T}_{max}$ [%]**
0	3.78	0.00
5	3.79	0.26
10	3.83	1.32
20	4.02	6.35
30	4.36	15.34

Since the value of $\Delta\tilde{T}_{max}$ evolves with time, it was decided to evaluate it at a given Fourier number. Doing so, the only remaining independent variables are Pe and the ratio of thermal conductivities. Fig. 2.7 shows the evolution of $\Delta\tilde{T}_{max}$ according to these two parameters. Data were extracted at a dimensionless time of $Fo = 10$ during the heating stage. This Fourier value was chosen because it was observed that the difference of temperature between sensors changes slowly for $Fo > 10$. Fig. 2.7 reveals that one can find the subsurface flow Peclet number as long as the difference of temperature is large enough since $\Delta\tilde{T}_{max}$ is nearly linearly dependent on Pe. $\tilde{k}$ merely changes the slope of the line function between Pe and $\Delta\tilde{T}_{max}$. Its impact is only observable for high values of Pe $(\text{i.e. } Pe \geq 0.02)$, but neglecting the ratio of conductivities can lead to error that are up to 20% when $Pe \approx 0.1$ and thus must not be completely ignored.

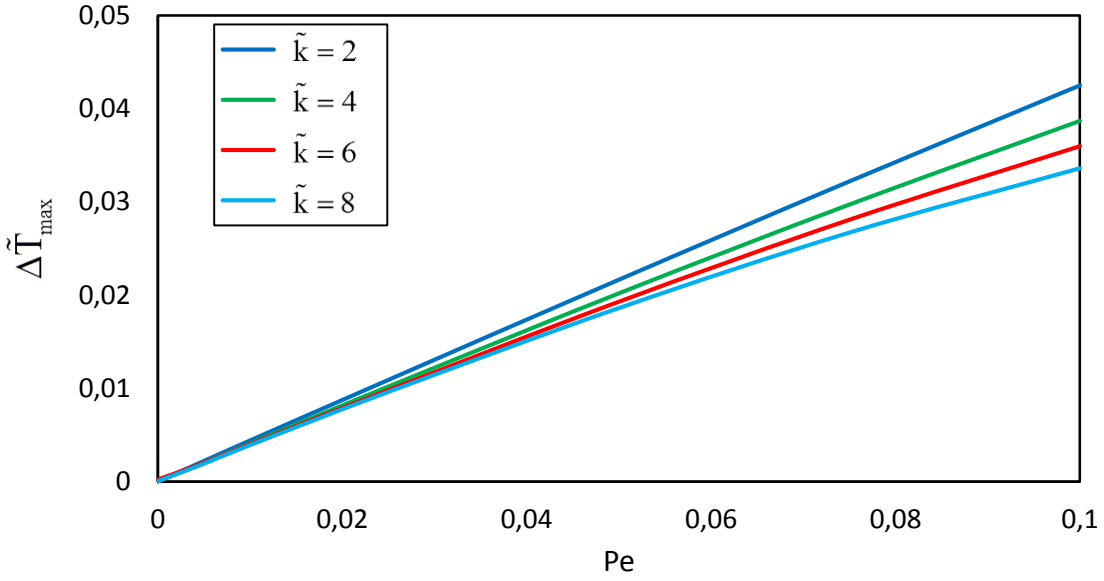

Figure 2.7 - Maximum dimensionless difference of temperatures on the borehole wall versus the flow Peclet number.

2.5.3 Evaluation of thermal conductivity

The ground thermal conductivity can be estimated during the recovery period by curve-fitting the evolution of the average borehole wall temperature $\overline{\theta}_b(\mathrm{Fo})$ calculated by a model to the one that is observed in the borehole temperature once it becomes uniform. To do that, it is approximated that the average temperature of the borehole wall is equal to the mean value of the three thermal sensors. Calculated temperature evolution can be obtained using a dimensionless ground function $G(\mathrm{Fo})$, that is used to determine the temperature increment during heat injection:

$$\overline{\theta}_b(\mathrm{Fo}) = \frac{q_0'}{k_{avg}} G(\mathrm{Fo}) \tag{2.14}$$

Once heat injection is stopped, the temporal superposition principle can be used to calculate $\overline{\theta}_b(\mathrm{Fo})$:

$$\overline{\theta}_b(\mathrm{Fo}) = \frac{q_0'}{k_{avg}} \left(G(\mathrm{Fo}) - G(\mathrm{Fo} - \mathrm{Fo}_{Heat}) \right) \tag{2.15}$$

where Fo_H is the Fourier number when heat injection is stopped.

2.5.3.1 Time needed for the temperature in the borehole to be uniform

Simulations were carried out to provide an estimation of the dimensionless time required to reach temperature uniformity in the borehole Fo_U once the heat source is turned off. The temperature uniformity criterion was arbitrarily set at 0.1°C everywhere in the borehole. Uniformity of temperature within the borehole is not necessarily reached when all three sensors have the same reading as the middle of the borehole could be warmer due to presence of the heat source. To circumvent this problem, it is possible to place a fourth sensor near the source to directly find the moment when the temperature is uniform or the results presented here can be used to get an estimate. The simulations showed that there is a logarithmic relation between Fo_{Heat} and Fo_U:

$$\mathrm{Fo}_U = q_0' \left(A_0 \ln(\mathrm{Fo}_{Heat}) + A_1 \right) \tag{2.16}$$

where A and B are functions of Pe and $\tilde{k}$. Table 2.6 provides the values of A_0 and A_1 for different sets of Pe and $\tilde{k}$. The time required for the temperature to become uniform during thermal recovery increases for fast flows, but remains relatively short for grounds with high thermal conductivity. The value of Fo_U can be estimated either from calculations done during the heating period or from regional data. In most cases, it is smaller than Fo_{Heat}.

Table 2.6 Values for parameters A_0 and A_1 as a function of conductivity and Peclet number.

$\tilde{k}$	Pe	A_0	A_1
2	0.001	4.5687	3.5467
	0.005	5.2177	2.9293
	0.01	7.1143	1.4616
	0.05	13.4187	-7.0897
	0.1	16.0432	-9.0012
4	0.001	3.8590	5.9664
	0.005	4.7474	4.0799
	0.01	5.5838	2.8738
	0.05	11.038	-5.1873
	0.1	13.342	-6.0213
6	0.001	3.4670	8.7863
	0.005	4.0878	7.6578
	0.01	4.3378	6.1265
	0.05	7.8746	1.2389
	0.1	9.3269	0.6742
8	0.001	3.3320	11.715
	0.005	3.9910	10.141
	0.01	4.3967	9.7387
	0.05	6.3037	3.7139
	0.1	7.3866	3.2603

2.5.3.2 Ground function for various Pe and $\tilde{k}$

Advection not only leads to different temperatures read by each sensor, it also alters the temporal development of the mean temperature value of these sensors. A high $\tilde{k}$ value means that the subsurface has a high thermal conductivity compared to the one in the borehole and as a result, heat quickly travels out of the borehole area. Thus the ratio of thermal conductivities also affects the mean temperature value of the borehole perimeter.

From Eq. (2.14), this implies that the G-function has to be adapted with Pe and $\tilde{k}$. This subsection offers a tool to estimate $G(Fo)$. Fig. 2.8 presents $G(Fo)$ for different values of Pe and of $\tilde{k}$, directly given by the numerical model. For short time-scales, while Pe has no effect on the G-function, $G(Fo)$ is highly influenced by $\tilde{k}$. The impact of $\tilde{k}$ is only observable for $Fo < 10$. Then, for longer time scales, advection comes in and the groundwater flow starts to dominate the heat transfer process over radial conduction. The critical Fourier Fo_c separating these two states highly depends on Pe. While $Fo_c \approx 10$ for flows of $Pe = 0.1$, this value increases up to $Fo_c \approx 250$ when $Pe = 0.025$. These critical values can be used to determine the limit of the pure conductive stage if one wants to use the line-source theory to deduce the effective thermal conductivity during the heating period. In spite of the presence of groundwater flows, typical TRT durations are not long enough for the system to reach a steady-state, unless the test is executed in an unusually high permeable aquifer $(Pe > 0.1)$. With the dimensionless time range used for this analysis, effects of convection on the G-function become apparent when $Pe \geq 0.02$. Not accounting for advection during TRT analysis leads to erroneous estimation of thermal conductivity when the flow Darcy velocity is higher than this value.

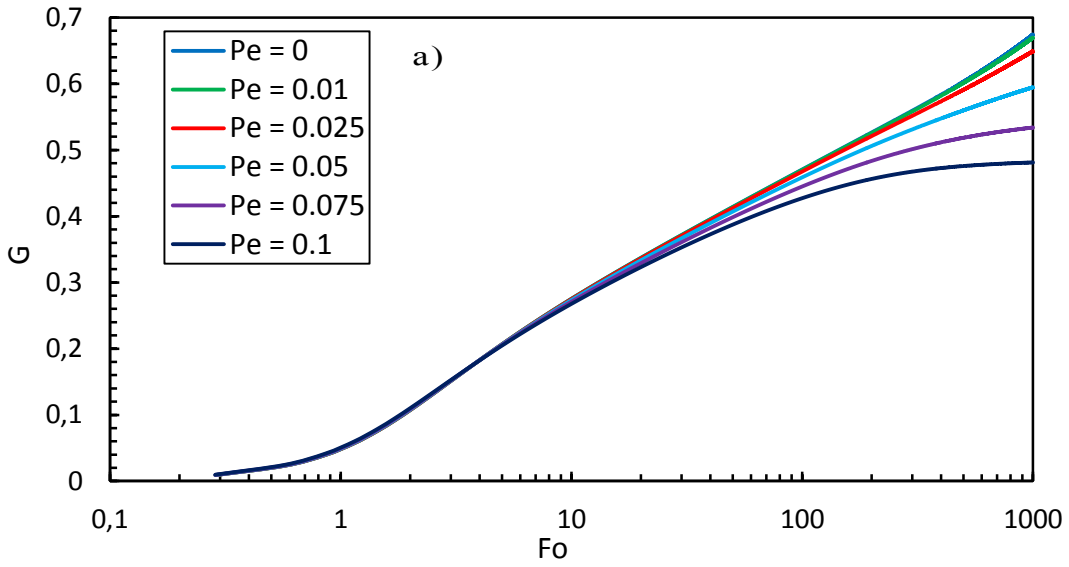

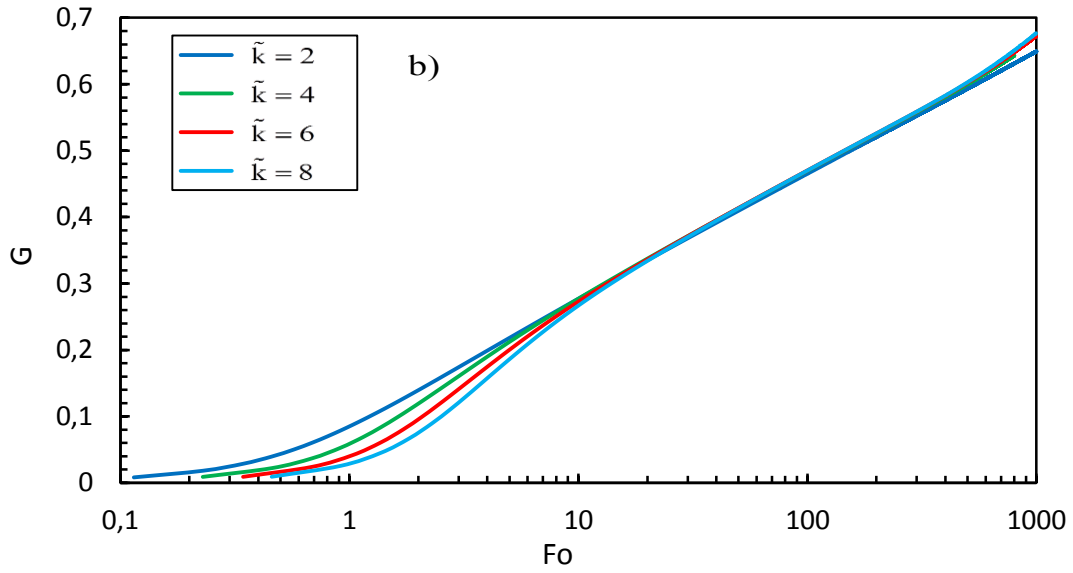

Figure 2.8 - Ground function for the TRT a) as a function of the Peclet number $(\tilde{k}=5)$, and b) as a function of the ratio of thermal conductivities (Pe=0.01).

2.5.4 Schematic step-by-step analysis procedure

Figure 2.9 presents a summary of the suggested analysis method in a step-by-step procedure. After the preliminary steps of choosing test parameters, the H/TRT can be executed and then analysed. As previously explained, it is relatively easy to quickly obtain a good estimate for the groundwater flow orientation ϕ from the H/TRT data. Once this evaluation is done, it is possible to extrapolate the dimensionless maximum difference of temperature $\Delta\tilde{T}_{max}$ on the borehole perimeter using trigonometry. This dimensionless parameter is linked to the flow velocity number and thus could be used to obtain the Peclet number. However, the relation between $\Delta\tilde{T}_{max}$ and Pe is affected by the ratio of thermal conductivities $\tilde{k}$, which is still unknown. Therefore, an iterative procedure is required and a guess has to be made on the ground thermal conductivity k_{avg}. This guess on k_{avg} allows users to convert time values into Fourier numbers Fo and to measure a temporary value for Pe. Following that, curve-fitting on $G(Fo)$ is needed to get a new value for the ground thermal conductivity. It is preferable to do this curve-fitting when the temperature in the borehole is uniform during thermal recovery since it decreases the impact of an erroneous

position for the heat source or the sensors due to the absence of heat transfer within the borehole. To find when the temperature in the borehole is uniform, a fourth sensor can be placed within the borehole or Table 2.6 along with Eq. (2.16) can be used. If the curve for the average borehole wall temperature observed in the field fits with the one calculated with $G(\mathrm{Fo})$, then the iterative process is complete and the values for Pe and $\tilde{k}$ are final. If not, another iteration is required, going back to the calculation of Pe.

The procedure was numerically tested for numerous situations. To mimic a resolution of 0.1 °C for the temperature sensors, numerical data were rounded to the nearest tenth. Fig. 2.10 shows the results of 25 H/TRT tests with different orders of magnitude for $\tilde{k}$ and Pe. The values for $\tilde{k}$, Pe, ϕ, q_0', r_b and t_{Heat} were randomly selected, but had to fit within a realistic range (Table 2.3). No more than three iterations were required for each test.

Thermal conductivity values determined by this procedure were all within a range of 10% of the input value in the numerical model as shown in Fig. 2.10a. The methodology has a tendency to underestimate the ground thermal conductivity because of the presence of the borehole which is only filled with water – the fluid thermal conductivity is lower than the ground thermal conductivity, hence the slight underestimation. The use of a cylinder-source model could circumvent the problem. Measurements for the Darcy velocity were accurate when $u_D > 10^{-7}\,\mathrm{m/s}$ as the measurement error was under ±10% for all situations involving such a flow (see Fig. 2.10b). Below that value of u_D, measurements yielded less precise results. The H/TRT might be unable to reveal the groundwater flow when it is too weak. Fortunately, for geothermal applications, it is not needed to know the groundwater flowrate with great accuracy in that range of Darcy velocity. Simply knowing that the flow is weak is good enough for sizing vertical heat exchangers when the velocity is small. Evaluations of the flow orientation (Fig. 2.10c) were relatively accurate when $u_D > 10^{-7}\,\mathrm{m/s}$. For slower groundwater flow, the direction estimation methodology is less effective. Obviously, the angle cannot be estimated when the setup cannot sense groundwater flow.

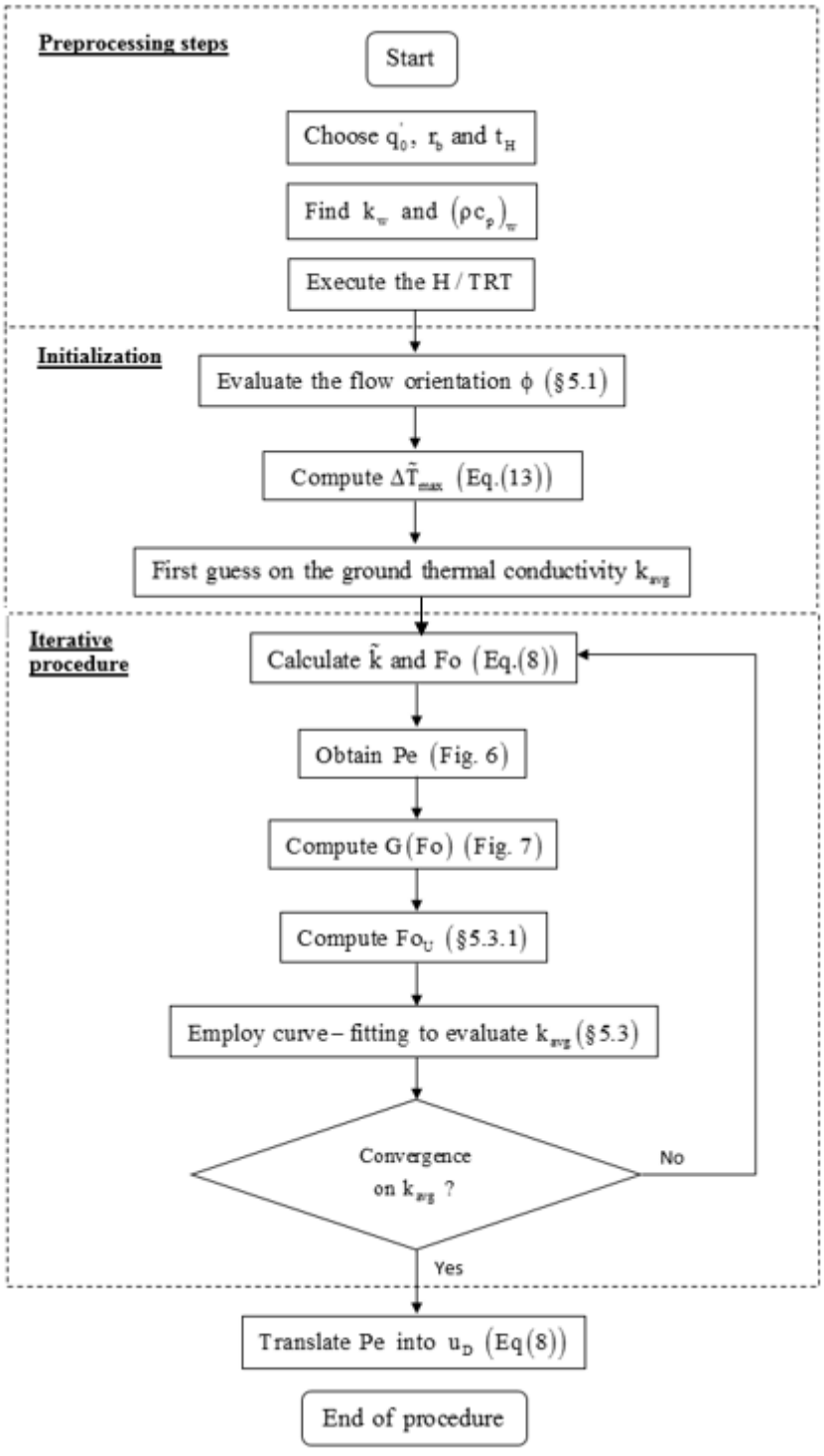

Figure 2.9 - Suggested flowchart for the H/TRT analysis procedure.

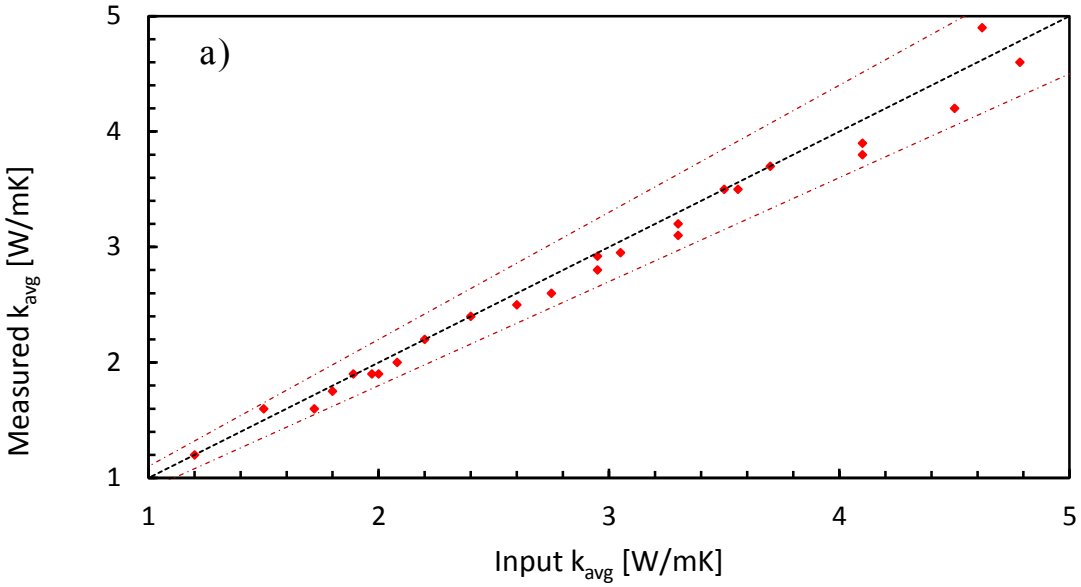
a)
Measured k_{avg} [W/mK]
Input k_{avg} [W/mK]
1
2
3
4
5

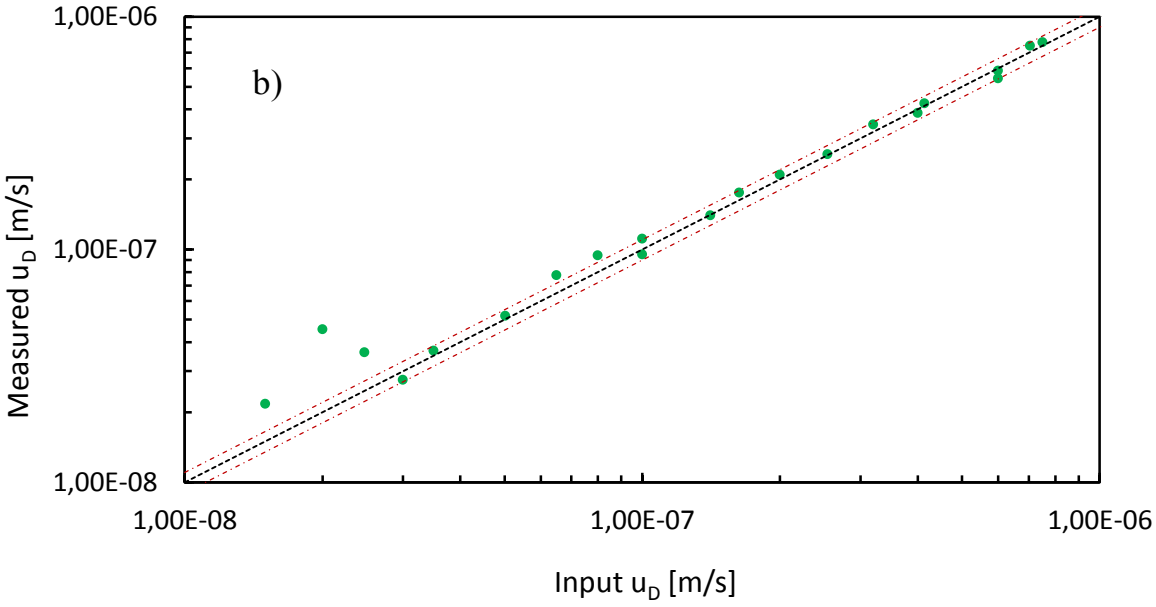
b)
Measured u_D [m/s]
Input u_D [m/s]
1,00E-06
1,00E-07
1,00E-08

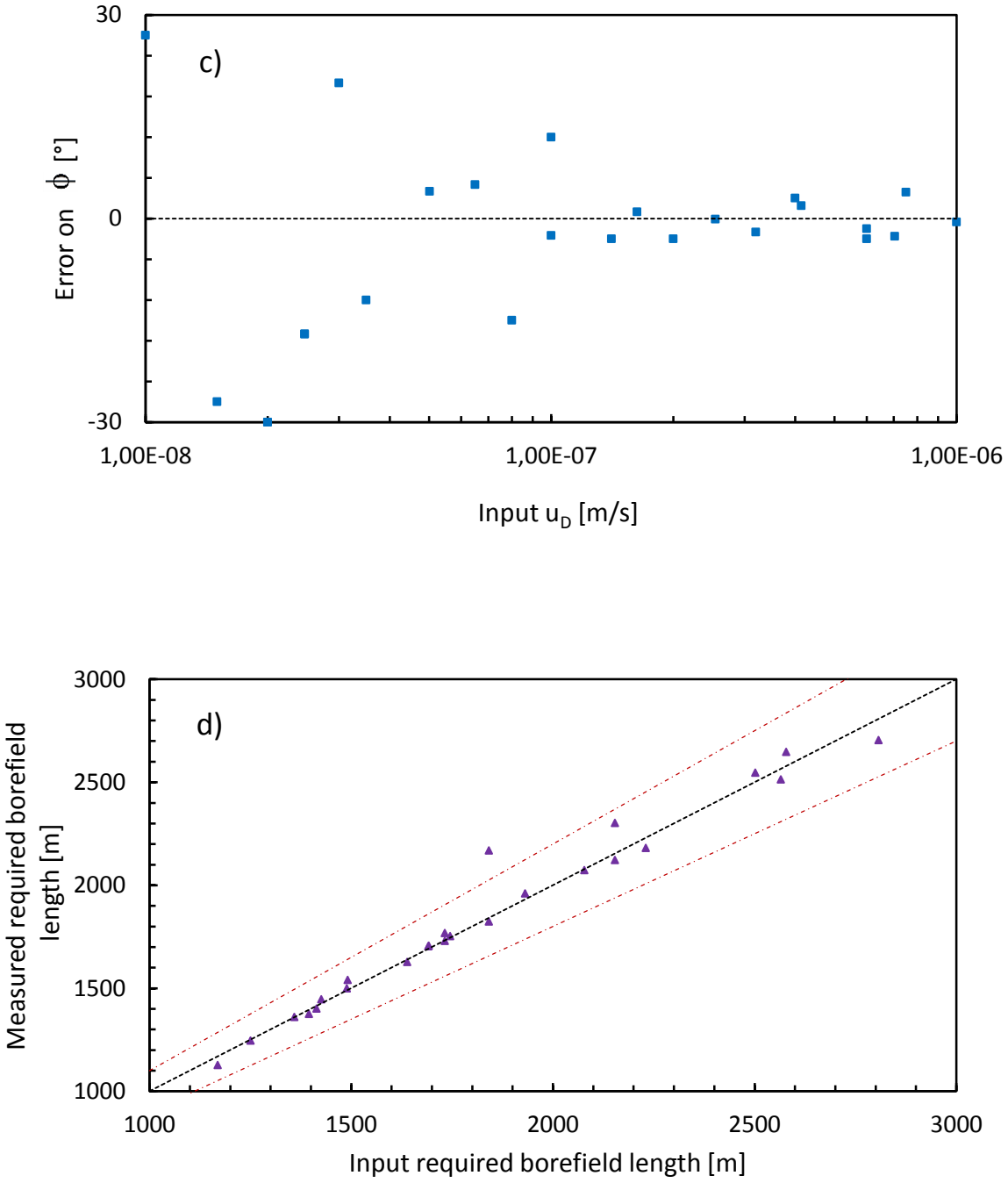

Figure 2.10 - Comparison between estimates of the parameters obtained from the H/TRT and their actual values for a series of random cases: a) subsurface thermal conductivity b) Darcy velocity c) flow orientation, and d) required borefield length. (Both values are equal when markers fall on the black dashed line. Red dashed lines correspond to an error of ±10%).

Table 2.7 Test case used for evaluation of required borefield length as a function of the ground parameters.

Variable	Value	Variable	Value
T_g	10°C	q_y	8 kW
$T_{f,avg}$	0°C	q_m	20 kW
r_b	0.075 m	q_h	30 kW
R_b	0.25 mK/W	N_x	5
τ_y	15 years	N_y	4
τ_m	2 months	B	4 m
τ_h	24 hours		

To assess the impact of the errors on the hydro-thermal ground parameters estimated from the above-mentioned H/TRT procedure, the overdesign of the borefield total length produced by these errors were determined using a spreadsheet that considers groundwater flow for the calculation of required length of geothermal borefield L [8]. Calculations were done using typical values of borefield characteristics (Table 2.7). The total BHE length was calculated both with input values (i.e. values considered as the right or real ones) of ground thermal conductivity, groundwater flow velocity and orientation and with their estimations (i.e., that obtained from the test). The required lengths calculated with both sets of values (i.e. real values versus those obtained from the test) are presented in Fig. 2.10d and were very similar. The borefield overdesign was more than 10% for only one simulation case, mostly because of a poor choice for the test parameters – the power input for the heating period, which only lasted 40 hours, was 20 W/m for that specific test. With proper test parameters (i.e. higher heat generation rate and longer heating period), the borefield overdesign is not critical and thus the H/TRT seem to offer a good tool for sizing geothermal borefields. For the heat injection rate, according to results, a power input superior to 30 W/m seems sufficient if the temperature probes have a resolution of 0.1°C. As for the duration of the heating period, a period longer than $Fo > 10$ is recommended to get a large difference of temperature between the sensors. Considering a minimal thermal conductivity of the ground around 1 W/mK and a maximal volumetric heat capacity close

to 3×10^6 J/m^{3}K, the minimal ground thermal diffusivity is approximately $\alpha \approx 3.33\times10^{-7}\ \mathrm{m^2/s}$. This means that, in a borehole with a radius of $r_b = 0.075\mathrm{m}$, the heat source has to be activated for at least 46 hours to be sure that the minimal Fourier number is reached.

2.6 Conclusions

This paper introduced a new configuration of H/TRT to simultaneously estimate the ground thermal and hydraulic properties. The setup uses three temperature sensors set around a heating cable in a borehole. Evolution of temperature is monitored by all sensors during both the heating period and the thermal recovery. A numerical model was used to evaluate the potential of the concept. With the help of tools given in the paper, the thermal responses of each sensor reveal the subsurface effective thermal conductivity, the groundwater flow velocity and its orientation. Knowing the flow properties is important for designing appropriate geothermal borefields. Since the tools provided are based on dimensionless scales, they offer flexibility regarding the heat injection rate, the duration of the heating period and the borehole dimensions. The amount of energy required by the TRT procedure does not exceed what is actually used by conventional TRTs. Moreover, the method is highly adaptable as it works for low power sources in geological settings that have low hydraulic conductivity. It is possible to execute it at various depths to find the distribution of ground properties, leading to better designs.

Numerical simulations were done to reproduce the heat transfer produced by the TRT for various conditions. Variations of the ground thermal conductivity, the groundwater flow velocity and orientation, the heat injection rate, the borehole radius and the duration of the heating period were considered for numerical validation of the system. Simulations disclosed that, in spite of the presence of advection, it is possible to deduce thermal conductivity by curve fitting the thermal response during thermal recovery. It is suggested to calculate thermal conductivity during the recovery. As for the parameters of the groundwater flow, they are estimated during the heating stage because they are measured via the differences of temperatures between the sensors. These gaps of temperatures are higher when the heat source is on. The creation of differences of

temperatures that are perceptible can be achieved with a power source of 60 W/m unless the flow is small enough to be neglected in the heat transfer process. However, for low Peclet numbers, it is possible that the setup is unable to sense any flow. Since thermal recovery is monitored, the total duration of the test might be higher than conventional TRTs.

The numerical model built for this study was 2D. Three-dimensional effects accounting for natural convection or geothermal temperature gradient could be investigated in future work. An additional work would be to establish the number of vertical measurements that would be needed in order to obtain a satisfactory vertical distribution of ground and groundwater flow properties. The model used a permeable boundary between the ground and the borehole, hence it does not consider the borehole thermal resistance, contrarily to traditional TRTs. Furthermore, an extensive sensitivity analysis of the variables, such as the position of the heat source and sensors, or the thermal properties for groundwater, would be helpful as there are many high uncertainties when working with ground properties. The suggested concept also needs to be tested in-situ and experimentally validated.

This work demonstrates the potential of the proposed TRT to reveal thermal and hydraulic ground properties while keeping the time, cost and equipment low. Development of thermal response tests accounting for groundwater flow should be pursued in the future to enhance the designing of geothermal borefields.

Chapitre 3 Article de revue

Titre

INVERSE HEAT TRANSFER APPLIED TO A CONCEPT OF HYDROGEOLOGICAL AND THERMAL RESPONSE TEST FOR GEOTHERMAL APPLICATIONS

Co-auteurs

Jean Rouleau, Louis Gosselin

Journal

International Journal of Thermal Sciences – Article soumis le 9 Septembre 2015

Résumé

Les tests de réponse thermique actuels, qui servent à mesurer la conductivité thermique du sol où on souhaite y implanter un champ de puits géothermiques, ne permettent pas d'évaluer ni la vitesse ni l'orientation des écoulements souterrains. Puisqu'ils influencent le transfert thermique se produisant entre un puits géothermique et le sol qui l'entoure, ces paramètres sont importants pour obtenir un dimensionnement idéal d'un champ géothermique. Dans le but de corriger ce défaut, un nouveau concept de test, où des sections de câbles chauffants injectent de la chaleur dans un puits, a été développé. Trois capteurs de température sont stratégiquement placés sur le pourtour du puits. Cet article applique au montage étudié des stratégies de résolution de problème inverse de transfert de chaleur pour identifier la conductivité thermique du sol, en plus de la vitesse et de la direction de l'écoulement souterrain. Le test proposé et la méthode d'estimation des paramètres employée y sont présentés. L'influence du point de départ de l'algorithme de résolution a également été étudié. Le travail présenté dans cet article a été effectué à partir de simulations numériques.

Abstract

Actual thermal response tests, used to estimate the subsurface thermal conductivity in the geothermal sector, do not provide any estimate on the velocity of the groundwater flow and its orientation. These parameters are important for sizing geothermal borefield, since they influence the heat transfer around a geothermal borehole and the surrounding ground. To correct this shortcoming, a test concept in which heating cable sections inject heat in a borehole has been developed. Three temperature probes are strategically located at the borehole edge. This paper applies inverse heat transfer strategies to this thermal response test concept in order to identify the ground thermal conductivity, as well as the groundwater flow velocity and its direction. The suggested thermal response test and parameters estimation methodology are detailed. The influence of initial guessed values for the three unknown parameters was also studied. The work presented in this paper was carried out by numerical simulations.

3.1 Introduction

Since ground-coupled heat pump (GCHP) systems have a lower environmental impact and higher energy efficiency than conventional heating and cooling systems, the demand for GCHP has expanded greatly during the last decades. In Canada, the utilization of geothermal energy has grown from 3 000 TJ in 2003 to 11 000 TJ in 2013 [4]. GCHP systems combine heat pumps with ground heat exchangers (GHE). Because the rate of exchange between a GHE and the undisturbed ground depends on the thermal properties of the ground, such as the thermal conductivity, the undisturbed ground temperature and its thermal diffusivity, a proper design of GHEs asks for the knowledge of these properties. In situ thermal response tests (TRTs) are used to measure the subsurface thermal properties. The transient evolution of the temperature of heated water circulating in a GHE is measured at the inlet and outlet of a trial GHE. With proper models, it is possible to deduce the ground thermal properties from this test [17][19][20].

As it is simple to use and provides good estimates, the analytical line-source model, based on Kelvin's line-source equation [50], represents the common choice of model to evaluate the ground thermal conductivity. However, many assumptions are made when using the line-source model, such as a homogeneous and isotropic ground, and a heat transfer from the borehole that is entirely conductive and purely radial. In practice, these hypothesis are not necessarily true, depending on the geological materials where the TRT is executed. Water located in a saturated aquifer can move through ground pores and generate a flow motion. If the mean velocity of this flow is relatively high, it will affect the heat transfer between the ground and the borehole. This usually does not affect too much the results of the TRT (i.e., measurement of conductivity) as the effect of advection is usually observed after a relatively long time. However, it would be necessary to know the groundwater flow velocity and direction in order to design the GHEs properly. Consequently, results derived from conventional TRT can be incomplete, even inaccurate, when there is groundwater flow around the boreholes [19][25][26]. While some models allow correcting the data read by standard TRTs to account for groundwater flows [27][29][32], these tests were not designed to yield significant information on groundwater flow.

The impact of groundwater flow on the performance of geothermal borefields has been studied over the last years [10][23][21]. Advection enhances heat transfer between the GHE and the subsurface, which means that shorter GHEs are needed to provide the same performance when there is groundwater flow – geothermal borefield designing models must therefore consider groundwater flows. In recent works, it has been demonstrated that with a moderate flow velocity, neglecting groundwater flow in design procedure can induce an overdesign of the borefield that can go up to 68% [8]. The direction of the flow is also an important parameter that can influence the optimal GHE layout [7]. Determining such parameters usually requires hydrogeological tests which might be prohibitive in terms of time and cost. Hence, there is a call for developing a combined hydrogeological and thermal test to acquire all the required estimates of ground properties in a single operation.

A concept of combined hydro-thermal response tests (H/TRT) has previously been proposed in chapter 2. This H/TRT is based on the work of Raymond et al. [37][38], using heating cable placed in a borehole to inject heat in the subsurface. With multiple temperature probes positioned in a horizontal plane around the cable, it is possible to find the thermal influence of groundwater flow and calculate its velocity and orientation. In a similar setup, Fic proved that the Darcy velocity of groundwater flow can be estimated from multiple temperature measurements as long as there is a nonzero horizontal temperature gradient in the ground [51].

Evaluating ground thermal conductivity from TRT data represents a typical example of inverse heat transfer problem (IHTP) [52]. This category of problems is usually solved by minimizing an error function between measurements and predictions of a model. The solution to inverse problems such as that of a TRT can depend on initial guess for each parameter, measurement uncertainties, control and placement of the heat source and temperature probes, power input for the source, etc. Moreover, using these techniques to estimate multiple parameters might prove to be difficult [53].

The purpose of this paper is to study the possibility of applying an inverse heat transfer method to an H/TRT. A parameter estimation methodology that determines thermal conductivity and groundwater flow parameters is presented. The concept is tested with a numerical model. The performance of the methodology is investigated as a function

of the estimation of the flow orientation, the initial guess of thermal conductivity and flow velocity used by the algorithm, the heat generation rate of the source and the measurements uncertainties.

3.2 H/TRT Modeling

3.2.1 H/TRT set-up

The proposed concept of TRT is adapted from the one introduced in the previous chapter, which is based on Refs. [37][38]. A heating cable is placed in a borehole to inject heat in the subsurface. The test is performed in a borehole before it is filled with grout. Fixed on the edge of the well, temperature sensors are then used to measure the evolution of the temperature in the borehole. The proposed setup is sketched in Fig. 3.1. Since the heat plume generated by the source will move towards the direction of the groundwater flow [54], a horizontal temperature gradient is created in and around the borehole. Each sensor will then monitor different temperature evolutions. An efficient analysis of these variations can potentially lead to an evaluation of the groundwater flow parameters, along with the ground thermal conductivity.

Probes are positioned at an interval of 120 degrees. The cable is positioned midway between two of them. This configuration maximizes the distance between the sensors. Larger separations produce larger differences of temperature, which facilitates the analysis of the test results. The monitoring of the temperature lasts for a certain time period of heating, followed by a recovery period (no heating) of equivalent duration. For this paper, the heating period and the recovery period were both three days.

In this paper, two important modifications were applied to the test. The main one is that instead of having the heat source at the center of the well, it was positioned on its edge, like the temperature probes. This move was made because it was deemed easier in practice to maintain the cable at the borehole perimeter. As errors on the location of the heat source cause inaccurate results when analysing TRT data, the difficulty of maintaining the cable at the center of the borehole represented a potential issue. Although this would probably result in uncertainties related to the angular position of the source, positioning the cable on the borehole wall eliminates uncertainties on its radial position and thus could reduce the

overall uncertainty on the cable position. The second change was making the frontier between the ground and the borehole impermeable. Many boreholes have casing inserted into their recently drilled sections. Casing provides support in weak formations to prevent it from caving-in. It is also beneficial for the lining of the well. Therefore, it is likely that TRTs be executed on borehole with casing. Not allowing groundwater to enter the well means that variations of temperature within the hole will be smaller, which could affect the test efficiency.

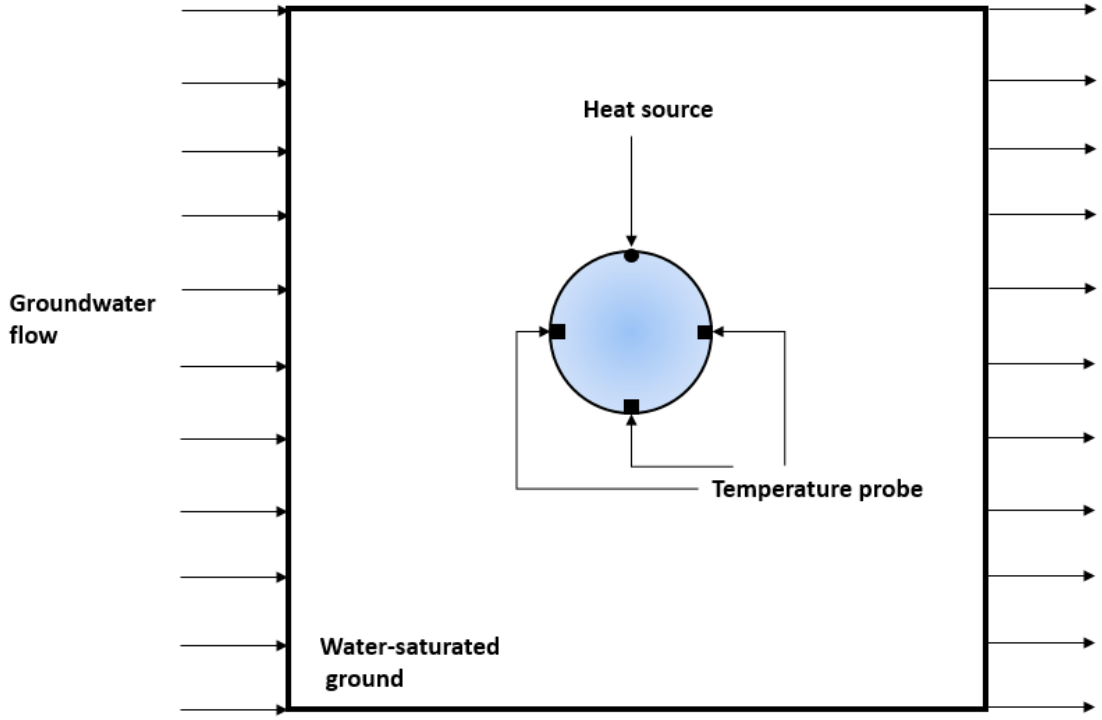

Figure 3.1 – Schematic representation of the modified H/TRT set-up to measure the ground thermal and hydraulic properties.

3.2.2 Governing equations

Two distinct heat transfer models are presented, inside and outside the borehole. The outside and inside temperature fields are related by the continuity of temperature and heat flux at the casing. Most models of GHE for TRT assume that the ground is a purely conductive medium. In the case studied here, this simplification is not applicable because of groundwater flow. The conservation of energy equation outside the borehole is:

$$\left(\rho c_p\right)_f\left(\chi\frac{\partial\theta}{\partial t}+\vec{u}\cdot\nabla\theta\right)=\nabla\cdot\left(k_{avg}\nabla\theta\right)\qquad\text{(outside)}\tag{3.1}$$

where:

$$\theta=T-T_g\quad,\quad\chi=\frac{\eta\left(\rho c_p\right)_f+\left(1-\eta\right)\left(\rho c_p\right)_s}{\left(\rho c_p\right)_f}\tag{3.2}$$

Thermal conductivity is equal to the weighted average of the water and dry ground properties. Effective thermal diffusivity is obtained by dividing the thermal conductivity of the porous medium to the volumetric heat capacity of water:

$$k_{avg}=\eta k_f+\left(1-\eta\right)k_s\quad,\quad\alpha_{eff}=\frac{k_{avg}}{\left(\rho c_p\right)_f}\tag{3.3}$$

The advection term $\vec{u}\cdot\nabla\theta$ is governed by the velocity vector $\vec{u}$. The characteristic Darcy's velocity was evaluated far from the borehole:

$$u_{r\to\infty}\equiv u_D=-\frac{\kappa}{\mu}\frac{\partial P}{\partial x}\tag{3.4}$$

As water gets closer to the borehole, its velocity and direction must change to get around the borehole wall, which is not permeable in the present model. The velocity vector can be expressed as the product between the characteristic Darcy velocity and a vector field:

$$\vec{u}\left(x,y\right)=u_D\cdot\vec{f}\left(x,y\right)\tag{3.5}$$

Since the borehole wall does not allow the groundwater flow to enter, the equation for the interior of the borehole does not contain advection:

$$\left(\rho c_p\right)_f\frac{\partial\theta}{\partial t}=\nabla\cdot\left(k_f\nabla\theta\right)\qquad\text{(inside)}\tag{3.6}$$

Eqs. (3.1) and (3.6) are related by the continuity of the physical fields at the wall:

$$\begin{aligned}\theta_o\big|_{r=r_b}&=\theta_i\big|_{r=r_b}\\ \left.\frac{\partial\theta_o}{\partial r}\right|_{r=r_b}&=\left.\frac{\partial\theta_i}{\partial r}\right|_{r=r_b}\end{aligned}\tag{3.7}$$

This formulation implies that the thermal resistance of casing is not considered. In order to limit the number of variables and to generalize results, the problem was solved with dimensionless variables:

$$\tilde{x},\tilde{y} \equiv \frac{x,y}{r_b}, \quad Pe \equiv \frac{u_D r_b}{\alpha_{eff}}, \qquad Fo \equiv \frac{t\alpha_{eff}}{r_b^2}, \quad \tilde{\theta} \equiv \frac{2\pi k_{avg}\theta}{q_0'} \tag{3.8}$$

Here, q_0' represents the heat generation rate of the heat source per unit length during the heating process. Based on data coming from [44], a range of possible values was considered for the simulations of this paper for each of the dimensionless numbers, see Table 2.3. Using the dimensionless scales, Eqs. (3.1) and (3.6) can be reduced to:

$$\chi \frac{\partial\tilde{\theta}}{\partial Fo} + Pe \cdot \vec{f}(\tilde{x},\tilde{y}) \cdot \tilde{\nabla}\tilde{\theta} = \tilde{k}\tilde{\nabla} \cdot \tilde{\nabla}\tilde{\theta} \quad \text{(outside)} \tag{3.9}$$

$$\frac{\partial\tilde{\theta}}{\partial Fo} = \tilde{\nabla} \cdot \tilde{\nabla}\tilde{\theta} \quad \text{(inside)} \tag{3.10}$$

where $\tilde{k} \equiv k_{avg}/k_w$ is the ratio of thermal conductivity (outside versus inside of the borehole). Four parameters influence the transient evolution of temperature: the ratio of thermal conductivities $\tilde{k}$, the Peclet number of the flow Pe, the direction of the flow ϕ (as it affects the vector field $\vec{f}(\tilde{x},\tilde{y})$) and the ratio of volumetric heat capacities χ. By using these equations, the following assumptions are made, as in the second chapter of this work:

(i) Local thermal equilibrium between water and dry ground is assumed;

(ii) Groundwater flow is assumed to be unidirectional and parallel to the ground surface. Furthermore, groundwater flow is supposed to be in steady-state and to be present everywhere in the domain;

(iii) The heat transfer is also assumed to be parallel to the ground surface, i.e. any vertical temperature gradient is neglected. This assumption is fairly good considering the short periods of time over which tests are performed [47].

(iv) All properties are assumed to be uniform and non-affected by temperature;

(v) Dispersivity is not considered in the model.

(vi) Natural convection inside the well is neglected. In spite of the presence of a heat source, there are several ways to cut off buoyancy-driven convection such as packers, perforated disks [38] or continuous heat cable [49]. Note that natural convection is also possible in the porous ground because the borehole wall is warmer than its surrounding [55]. This phenomenon is not considered here.

3.2.3 Numerical model

A numerical model was built with a finite element software [14] to reproduce the two-dimensional domain displayed in Fig. 3.1. The numerical model has the shape of a square (ground) with a hole at its center (geothermal well). The length of the square is 80 times the borehole radius. An infinite element zone was added to the model boundary. The mesh of the model has 15,102 unstructured triangular elements and follows the same pattern as previously shown in Fig. 2.2. Since temperature gradients should be maximal around the borehole, the elements of the mesh are mainly concentrated in this area of the domain.

Mesh and time-step independence were thoroughly tested. Mesh independence was declared when doubling the number of elements in the domain yielded a relative discrepancy of less than 1% on the average temperature of the probes for every time-step in the considered range. Time stepping needed to solve the energy equation is automatically chosen by the software while simulating, adjusted with a relative tolerance of 10^{-3}.

Throughout the simulations, properties of water remained constant – it was the properties of ground matrix that were varied between each simulation to consider different types of geological environments. Table 2.2 presents the value used for the properties of water.

The initial condition was a zero relative temperature $\theta = 0°C$ everywhere in the domain. Temperature at the infinite zone boundaries were also fixed at $\theta = 0°C$ as they are considered far from the TRT radius of thermal influence. The electrical cable is represented by a heat point source – a radial heat flux was imposed at the node corresponding to the prescribed position of the cable on the borehole wall. Concerning this boundary, a "no slip" wall condition is imposed so that the casing prevents groundwater flows to enter the borehole.

To achieve different levels of groundwater flow, the pressure difference between the left-side and the right-side boundaries of the domain was varied.

On a desktop computer with a 3.4 GHz processor and 16 Go of RAM, a simulation of a H/TRT required approximately three minutes. Keeping this amount of time low is necessary when the purpose of the model is to be repetitively used in an optimization algorithm, explaining the authors' preference for a two-dimensional model over a three-dimensional.

3.3 Inverse heat transfer approach

The configuration of H/TRT described in Section 3.2 gives the temperature at three different points in the domain. One needs to translate these temperature curves into the evaluation of unknown parameters. This represents an inverse heat transfer problem. Inverse heat transfer problems are usually solved by minimizing the error between measurements and model predictions. Sensitivity analysis can also be useful in inverse problem to understand the importance of each parameter on the value of the objective function.

3.3.1 Error function

The simplest choice for an error function to be minimized in this inverse problem is the sum of squares of deviations, or the *ordinary least squares norm*. In case where multiple sensors are used to monitor temperature with enough measurements to consider temperature data as being continuous, this function is written as:

$$S\left(\vec{P}\right)=\sum_{m=1}^{M}\int_{0}^{t_{test}}\left[Y\left(x_p,y_p,t\right)-T\left(x_p,y_p,t,\vec{P}\right)\right]^2 dt \qquad (3.11)$$

where $\vec{P}\equiv\left[Pe,\phi,\tilde{k},\chi\right]$ is the vector of unknown parameters, $T\left(x_p,y_p,t,\vec{P}\right)$ is the estimated temperature at $\left(x_p,y_p\right)$ according to the current estimate of $\vec{P}$, $Y\left(x_p,y_p,t\right)$ is the measured temperature at $\left(x_p,y_p\right)$ and M is the number of sensors – in this case, M = 3. The matrix T is calculated by the numerical model.

If the IHTP involves the evaluation of a large number of parameters, oscillations of the solution may occur due to the presence of measurement errors. In such cases, for the reduction of instabilities, it is suggested to employ regularization, e.g. Tikhonov's regularization [56]. An alternative approach is the use of Alifanov's Iterative Regularization Methods. In the present work, since the number of unknowns was relatively small, and based on the numerical tests that we performed, it was decided to use Eq. (3.11) without regularization.

3.3.2 Error minimization iterative procedure

The *fmincon* solver from Matlab optimization toolbox [57] was used to minimize Eq. (3.11). *fmincon* attempts to find a minimum within bounds of a scalar nonlinear function of several variables starting from an initial estimate. The solver is based on interior trust region methods for nonlinear minimization. This method uses a barrier function to encode the original minimization problem into a sequence of approximate problems that are easier to solve. To find the solution, the algorithm uses either a direct step or a conjugate gradient step at each iteration. For more details, this method is described in [58][59][60]. Matlab was coupled with the numerical model from COMSOL to simulate TRTs at each iterative step. Parameters to identify by the inverse problem were scaled to fit in a range from zero to one. The solver was constrained into a solution within that range, based on Table 2.3.

The optimization routine requires stopping criteria for the algorithm:

- Maximum number of iteration: 1000
- Maximum number of function evaluations: 3000
- Tolerance on $\vec{\mathbf{P}}$ (xTol): 10^{-5}
- Error function tolerance (FunTol): 10^{-6}
- Nonlinear constraint tolerance: 10^{-6}

Usually, the solver stopped by the changes of the vector of parameters $\vec{\mathbf{P}}$ (xTol). Since the parameters are scaled between zero and one, a tolerance of 10^{-5} on the changes of the parameters correspond to a termination tolerance set between 0.001% to 1%.

3.3.3 Sensitivity analysis

Before executing parameters estimation, it is useful to identify the most important parameters of the problem and the relationships between them. Knowing this leads to improved optimization strategies.

3.3.3.1 Ratio of volumetric heat capacities

Table 2.3 shows how limited the typical range of possible values is for χ – it varies from 0.55 to 0.75. This narrow range considerably reduces the influence of χ on the heat transfer process. It was verified that the observed differences of temperature during H/TRTs with $\chi = 0.55$ and $\chi = 0.75$ are not overwhelmingly high. For example, with $\tilde{k} = 2$, $Pe = 10^{-3}$, $q_0^{'} = 80 W/m$ and $r_b = 0.05 m$, the value of the error function between $\chi = 0.55$ and $\chi = 0.75$ was $S(\vec{P}) = 1.525 \cdot 10^6 K \cdot s$. Considering that the test lasted for six days and that there were three sensors, such a value of the error function translates into an average difference of temperature of roughly 1 K between the two cases. Over the duration of the test, the sensors read an average of $\bar{\theta} = 13K$ and thus while the difference of temperatures caused by a wrong value for the ratio of volumetric heat capacities is observable, the thermal response of the setup is relatively not very sensitive to χ. Other scenarios were tested with similar conclusion. Moreover, as mentioned before, volumetric heat capacities can be relatively well estimated during drilling. Therefore, it has been determined that obtaining a good estimate of χ with the H/TRT is not primordial and thus this parameter was eliminated from the estimation technique described in this paper. A value of $\chi = 0.65$ was retained for the other simulations.

3.3.3.2 Ratio of thermal conductivities

The ratio of thermal conductivities $\tilde{k} = k_{avg} / k_w$ is known to be the primary parameter to be deduced. To understand the impact of this parameter on the objective function, the variation of $S(\vec{P})$ was measured for different values of $\tilde{k}$ within the range provided in Table 2.3. In order to calculate an error function, there was a need to compute a measured temperature

matrix Y. This matrix was generated with $\tilde{k} = 4$, $Pe = 0.05$ and $\phi = 90°$. Following the creation of matrix Y, numerous matrices T of estimated temperatures were calculated by the numerical model for different value of $\tilde{k}$. The error function $S(\vec{P})$ was then computed for each of these values of thermal conductivity. This operation was repeated for three distinct values of Pe. Since the true value of $\tilde{k}$ was 4 – the objective function should be minimal near this point. Indeed, it is the case in Fig. 3.2. There is clearly a single minimum for the least squares norm located at $\tilde{k} = 4$ for all three values of Pe. This demonstrates that a wrong assessment of the flow does not necessarily lead to inaccurate estimation of thermal conductivity. The objective function varies from about 2×10^7 to zero depending on $\tilde{k}$. The thermal conductivity parameter has a high influence on $S(\vec{P})$.

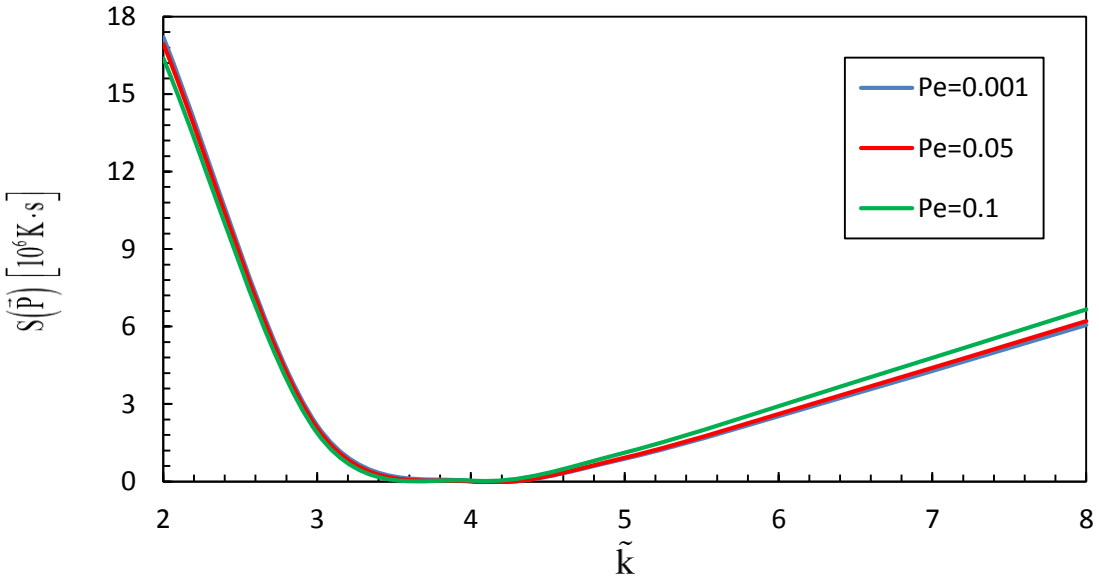

Figure 3.2 – Influence of $\tilde{k}$ on the objective function for different Peclet numbers, with $\phi = 90°$.

3.3.3.3 Peclet number

Figure 3.2 shows that the variations of the error function as a function of the Peclet number is relatively small compared to the ones induced by $\tilde{k}$. Consequently, the H/TRT is less sensitive to Pe than to $\tilde{k}$. The operations executed to draw Fig. 3.2 were repeated for the Peclet number Pe: sets of estimated temperature T were computed from the model for different flow velocities and the corresponding error function was generated. Instead of

setting the flow orientation as a constant, it was the ground thermal properties that were kept unchanged – the thermal conductivity was fixed at the true value of $\tilde{k} = 4$. The manipulation was done for five different flow directions. The results are displayed in Fig. 3.3 and confirm that the error function is less dependent on Pe than on $\tilde{k}$. While $S(\vec{P})$ can go up to $\sim 2 \times 10^7$ when changing the thermal conductivity, it can only reach a maximal order of magnitude of 10^5 when Pe changes. Besides, for some curves, the minimum for the objective function is not so clear. Contrarily to the thermal properties, it could be difficult to evaluate the flow velocity norm with the proposed setup. The relatively short duration of the test restricts the influence of the groundwater flow since the repercussion of advection increases with the time. Therefore, the studied TRT is less altered by groundwater flow than GHEs really are in operations.

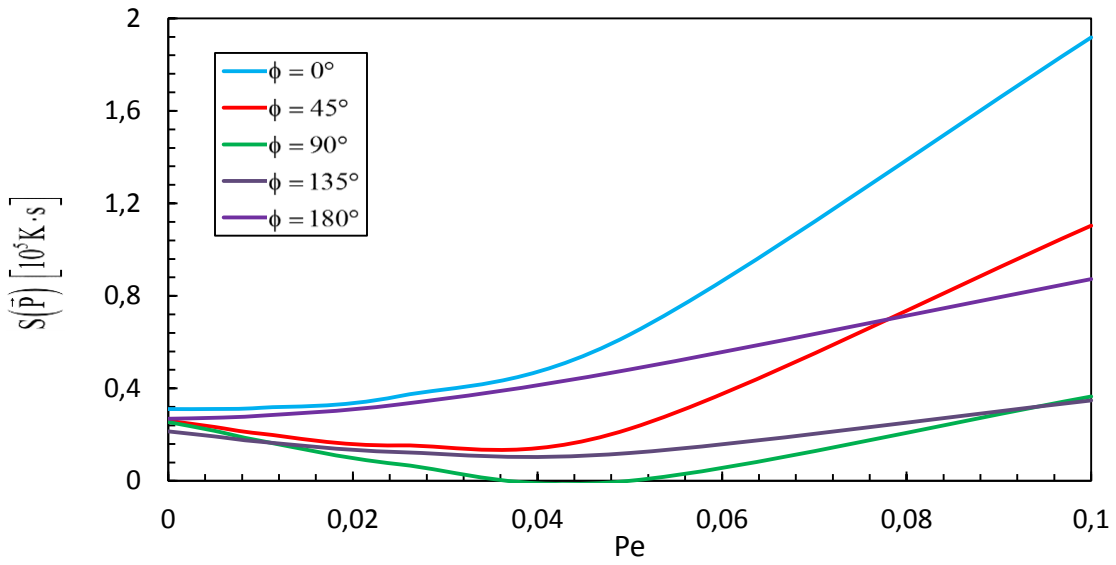

Figure 3.3 – Influences of Pe on the objective function for different flow orientations, with $\tilde{k} = 4$.

3.3.3.4 Flow orientation

The influence of the flow orientation ϕ on $S(\vec{P})$ can be estimated by comparing the five curves of Fig. 3.3. Likewise to the flow velocity, the largest gap between the four lines has an order of magnitude of 10^5 and thus, the flow orientation influence is less than the one of the thermal conductivity. Another observation that is visible from Fig. 3.3 is that the importance of ϕ increases with the flow velocity. For cases where Pe is close to zero, each

curve leads to similar values for the error function - the direction of the groundwater flow is nearly insignificant in these situations. However, at high Peclet, considerable discrepancies are seen between the curves. In short, the thermal sensitivity to ϕ depends on Pe. Accordingly, it should be easier to find the flow orientation when water is flowing at a fast pace, i.e. $\mathrm{Pe} \geq 0.01$.

3.3.4 Parameter estimation strategy

Different strategies are possible to solve the inverse problem and identify the missing parameters. For example, the missing parameters can be found simultaneously or one-by-one. This subsection presents a series of preliminary tests that have been performed to characterize these approaches in terms of calculation time, accuracy and stability, and eventually select the most promising one for the rest of the paper.

As presented earlier, three parameters have to be found. Table 3.1 summarizes results of parameter estimations according to the number of parameters estimated simultaneously when minimizing the error function. This investigation was accomplished for three values of the Peclet number, i.e. Pe = 0.01, 0.05 and 0.1. From Table 3.1, it can be observed that determining the three unknown parameters simultaneously in a single optimization generally provided unreliable measurements for the groundwater flow velocity and orientation. At moderate and high Peclet, the relative error on Pe is close to 100%. The only parameter that can be properly evaluated with the three-parameter minimization is the thermal conductivity, which has a large influence on $\mathrm{S}\left(\vec{\mathrm{P}}\right)$ as previously shown. Calculating all the parameters in a single minimization worked better when Peclet was small. It should be noted that three-parameter optimization runs also required large computational times (nearly five times longer than the other approaches described below).

Next, a solving procedure that divides the estimation into sequential steps was tested as shown in Table 3.1. Section 2.5.1 showed that with a similar setup, it was relatively straightforward to estimate the flow direction ϕ by looking at the temperature reported by the probes since the heat plume is aligned in the direction of the flow, and trigonometric relations were developed to estimate ϕ. Knowing this, one possible strategy

is to use a two-parameter simultaneous estimation of $\tilde{k}$ and Pe with a given value for ϕ. Because one of the sensors is positioned at a location farther from the heat source than the two others, the value of its temperature data must be adjusted for the direct evaluation of the flow orientation. This scaling was achieved with a single simulation of a scenario with no flow, providing a ratio of temperatures $CF = \theta_{\text{close sensor}} / \theta_{\text{far sensor}}$ (no flow) strictly caused by the difference of distances between the probes and the source (i.e., not by the groundwater flow). This ratio can be used as a correction factor CF when measuring ϕ:

$$\theta'_{\text{far sensor}} = \theta_{\text{far sensor}} \times CF \tag{3.12}$$

It was found that changes of the correction factor are negligible when varying $\tilde{k}$, Pe, ϕ, q'_0 and r_b, in such a way that CF can be assumed as first approximation to be a function of time only. Once a value for the flow orientation is obtained, it can be injected into the two-parameter estimation to find $\tilde{k}$ and Pe. With this scheme, only one optimization run is necessary to solve the parameter estimation problem. Table 3.1 shows that this approach proved to provide satisfactory results, with a low computational burden. Therefore, this approach was retained for the rest of the paper.

Table 3.1 Solution to the inverse heat transfer problem using different numbers of parameters in a single optimization.

Number of parameters estimated in each optimization	Peclet number	Relative error on $\tilde{k}$ [%]	Relative error on Pe [%]	Absolute error on ϕ [°]	Number of simulations
1	**0.01**	-0.82	-69	11	26
	0.05	-3.1	12	5.6	25
	0.1	1.5	-5.6	9.0	21
2	**0.01**	0.0	150	11	25
	0.05	-3.4	8.6	5.6	21
	0.1	-0.50	4.4	9.0	26
3	**0.01**	0.82	11	13	45
	0.05	0.68	-98	130	92
	0.1	0.50	-96	-110	105

3.4 Impacts of initial guess

In this section, the effect of the initial guess for $\vec{P} \equiv \left[Pe, \phi, \tilde{k} \right]$ on the resolution of the inverse problem is explored. Initial guess can influence both the accuracy of the parameter estimation and the computational times required by the algorithm.

3.4.1 Influence of flow orientation uncertainty

As described in Section 3.3, the first step of the proposed procedure is to guess the direction of the flow by comparing the temperature data from the three sensors. Since the second part of the algorithm uses the flow orientation for estimating thermal conductivity and flow velocity, an erroneous evaluation of ϕ might lead to inaccurate estimates for the other two parameters. It is thus important to assess the accuracy of the methodology to evaluate correctly the flow orientation and the impact that the error on this value has on resulting value for $\tilde{k}$ and Pe. First, the correctness of the guess on ϕ was verified for numerous flow orientations as shown in Fig. 3.4. This exercise was performed with a power of 40 W/m for the heat source and a ground thermal conductivity of $\tilde{k} = 8$. These values were chosen since they represented to worst scenario, leading to small temperature differences between the sensors (low power, high conductivity). If one can find the flow direction with this situation, ϕ estimates can only be better with larger power or lower conductivity. Fig. 3.4 shows that it is difficult to find ϕ when Peclet is low $\left(Pe \leq 0.01 \right)$. When $Pe \leq 0.01$, the inaccuracies for the approximation of the flow orientation can go up to $\pm 60°$. For higher Peclet, the accuracy is better, with errors within a range of $\pm 30°$.

Next, we assessed the effects of a wrong guess of ϕ on the estimation of the two other parameters. Fig. 3.4 showed that the error is usually greater when Peclet was small, but groundwater flow being slower in that range of Peclet also means that the flow orientation loses its impact on the error function $S\left(\vec{P}\right)$ and thus errors on ϕ should not be problematic for the estimation of $\tilde{k}$ and Pe. When Peclet is high, the methodology to evaluate the flow orientation is relatively accurate and should also have minimal influence on the two-parameter optimization. Fig. 3.5 compares the measurements of $\tilde{k}$ and Pe obtained with different values for the estimation of ϕ. In other words, values of ϕ around

the real one were fed to the two-parameter solver in order to verify that the values of $\tilde{k}$ and Pe returned by the solver would be acceptable even when ϕ is not exactly equal to its true value. The maximum error for the flow orientation was calculated by adding the maximum possible error on ϕ as prescribed by Fig. 3.4 ($\Delta\phi_{max} = \pm 60°$ when $Pe \leq 0.01$, otherwise $\Delta\phi_{max} = \pm 30°$) to the true value of ϕ. Results in Fig. 3.5 revealed that the estimations of $\tilde{k}$ and Pe were acceptable, even when the value of ϕ was uncertain.

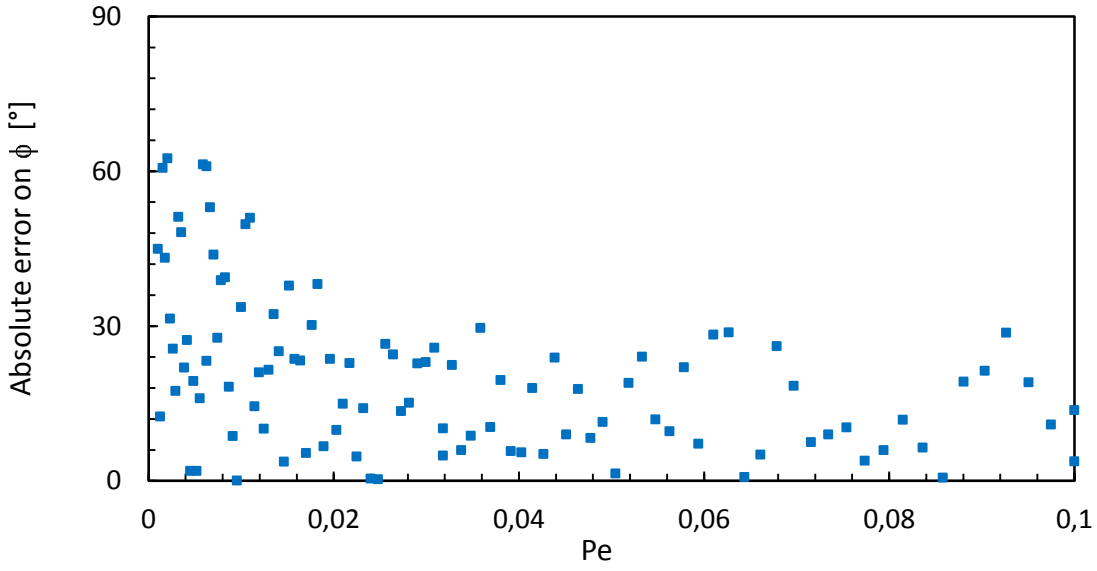

Figure 3.4 – Error on the estimated flow orientation according to the Peclet number.

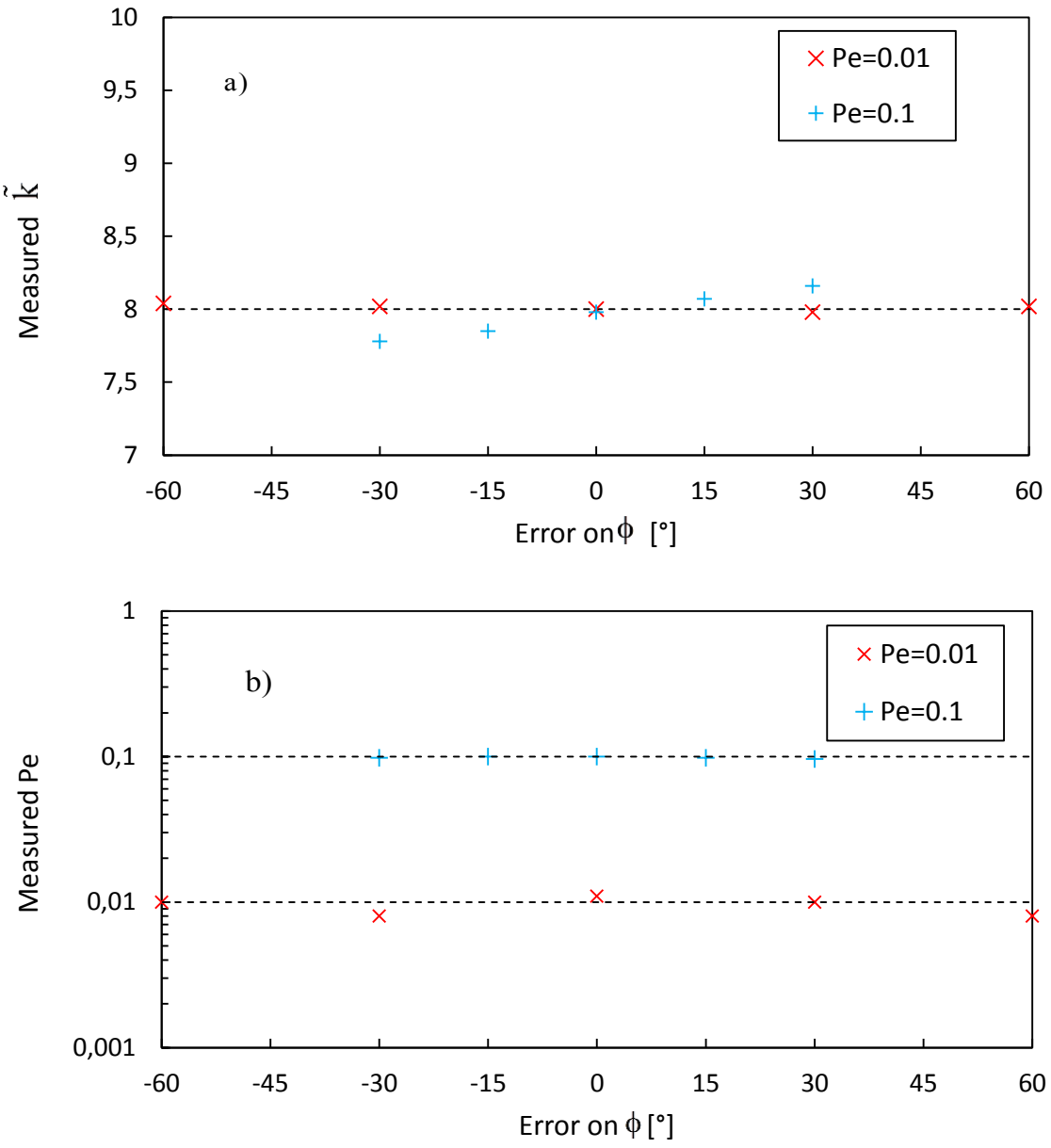

Figure 3.5 – Effects of an error on the estimation of ϕ on the measurement of: a) $\tilde{k}$, and b) Pe. "True" values are indicated by the black dashed line.

3.4.2 Influence of the initial guess for conductivity and Peclet number

The impact of the algorithm starting point $(\tilde{k}, Pe)$ on the iterative procedure was examined for two different cases: one where Pe was high $(Pe = 0.08)$ and another where Pe was lower $(Pe = 0.01)$. For each case, the algorithm was used to find the actual values of the

unknown parameters with ten different initial guesses for $(\tilde{k}, Pe)$ with the real value of the flow orientation. To ensure that the starting points covered all possible situations, we included the middle point of the parameter domain $(\tilde{k} = 5, Pe = 0.05)$, the four extreme points $(2, 0.001), (2, 0.1), (8, 0.001)$ and $(8, 0.1)$, plus five other initial guesses randomly selected. Solutions to the inverse problem from these initial guesses are presented in Table 3.2. There seems to be no correlation between the initial guesses and the accuracy of the parameter estimation procedure, or its computational times. The number of simulations needed by the solver varies between 15 and 65, which keeps the overall computational time within acceptable limits. For the rest of this paper, the starting point $(5, 0.05)$ was taken.

Table 3.2 Evaluation of the ratio of thermal conductivities $\tilde{k}$ and the groundwater flow Peclet number Pe for multiple initial guesses.

True values for $(\tilde{k}, Pe)$	Initial guess of $(\tilde{k}, Pe)$	Estimated values for $(\tilde{k}, Pe)$	Number of simulations required
(4.00, 0.080)	(2.00, 0.001)	(4.06, 0.072)	40
	(2.00, 0.10)	(4.01, 0.079)	40
	(3.20, 0.015)	(3.98, 0.078)	26
	(3.80, 0.030)	(3.98, 0.079)	49
	(4.40, 0.080)	(4.01, 0.074)	28
	(5.00, 0.050)	(3.98, 0.078)	21
	(6.20, 0.020)	(3.98, 0.079)	18
	(6.80, 0.060)	(3.98, 0.077)	41
	(8.00, 0.001)	(3.98, 0.082)	29
	(8.00, 0.10)	(3.98, 0.079)	26
(4.90, 0.010)	(2.00, 0.001)	(4.90, 0.0010)	35
	(2.00, 0.10)	(4.94, 0.008)	31
	(3.20, 0.015)	(4.94, 0.014)	41
	(3.80, 0.03)	(4.92, 0.0040)	24
	(6.80, 0.06)	(4.92, 0.0010)	36
	(5.00, 0.05)	(4.93, 0.0010)	20
	(6.20, 0.02)	(4.93, 0.0080)	37
	(7.00, 0.01)	(4.92, 0.0070)	53
	(8.00, 0.001)	(4.92, 0.019)	28
	(8.00, 0.10)	(4.91, 0.0060)	56

3.5 Performance of the estimation methodology

This section evaluates the performance of the parameter estimation methodology described previously. It also discusses the importance of the main TRT variables, such as the heat generation rate and the uncertainty on the temperature measurements. H/TRTs were simulated with the numerical model using values for the three unknown parameters which were considered to be the real ones. Each of these simulations generated an "exact" temperature vector $\vec{Y}_{ex}$ for each sensor, corresponding to the measurements that would be performed in situ in practice. These temperature vectors were combined into array $\mathbf{Y_{ex}}$. Since real measurements contain errors, an error term was added to $\mathbf{Y_{ex}}$ for a realistic representation of a H/TRT:

$$\mathbf{Y} = \mathbf{Y}_{ex} + \sigma\boldsymbol{\omega} \tag{3.13}$$

where σ is the standard error of measurements and $\boldsymbol{\omega}$ an array of pseudo-random variables with a normal distribution, zero mean and unitary standard deviation. Once the array of simulated temperature measurements containing errors $\mathbf{Y}$ is obtained, the ground parameters can be estimated by solving the inverse problem. For this work, the chosen test duration is six days (three days of heating, three days of thermal recovery) and the borehole radius remained constant at r_b = 0.05 m.

The performance of the concept is investigated by observing how accurate the estimations are for the ground thermal conductivity, the groundwater flow velocity and its orientation. To understand the effects of the precision of these estimations on geothermal field design, the estimated variables were also translated into a total GHE length needed for the borefield with the help of a borehole sizing model that considers groundwater flow [8]. Ground properties, borehole design, borefield characteristics and building loads that were used for this are listed in Table 2.7. Data are considered as representative of a hypothetical geothermal system designed for a medium-sized commercial building in Quebec City, Canada. The total GHE length was calculated both with "true" values of ground thermal conductivity, groundwater flow velocity and orientation and with their estimations obtained by solving the inverse problem as proposed here. Then, the relative difference between these two lengths was calculated.

The procedure was numerically tested for numerous scenarios. Using another estimation methodology, the previous version of H/TRT was tested for 25 scenarios

combining different values of $\tilde{k}$, Pe, ϕ. These 25 cases were considered again in the present paper to test the proposed methodology, with sensors that have an absolute uncertainty of $\pm 0.1°C$. The resulting value of thermal conductivity determined by solving the inverse problem was compared to the real value (Fig. 3.6a). The same was done for the Darcy velocity (Fig. 3.6b) and borefield required total length (Fig. 3.6c). Note that the ability of the suggested methodology to assess flow orientation was presented previously, see Fig. 3.4.

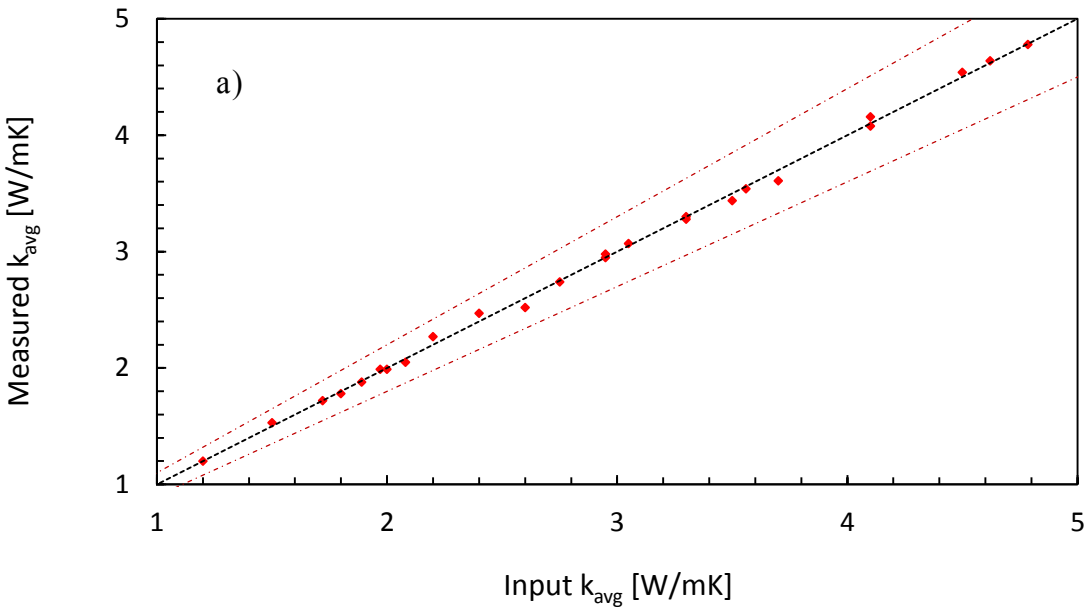

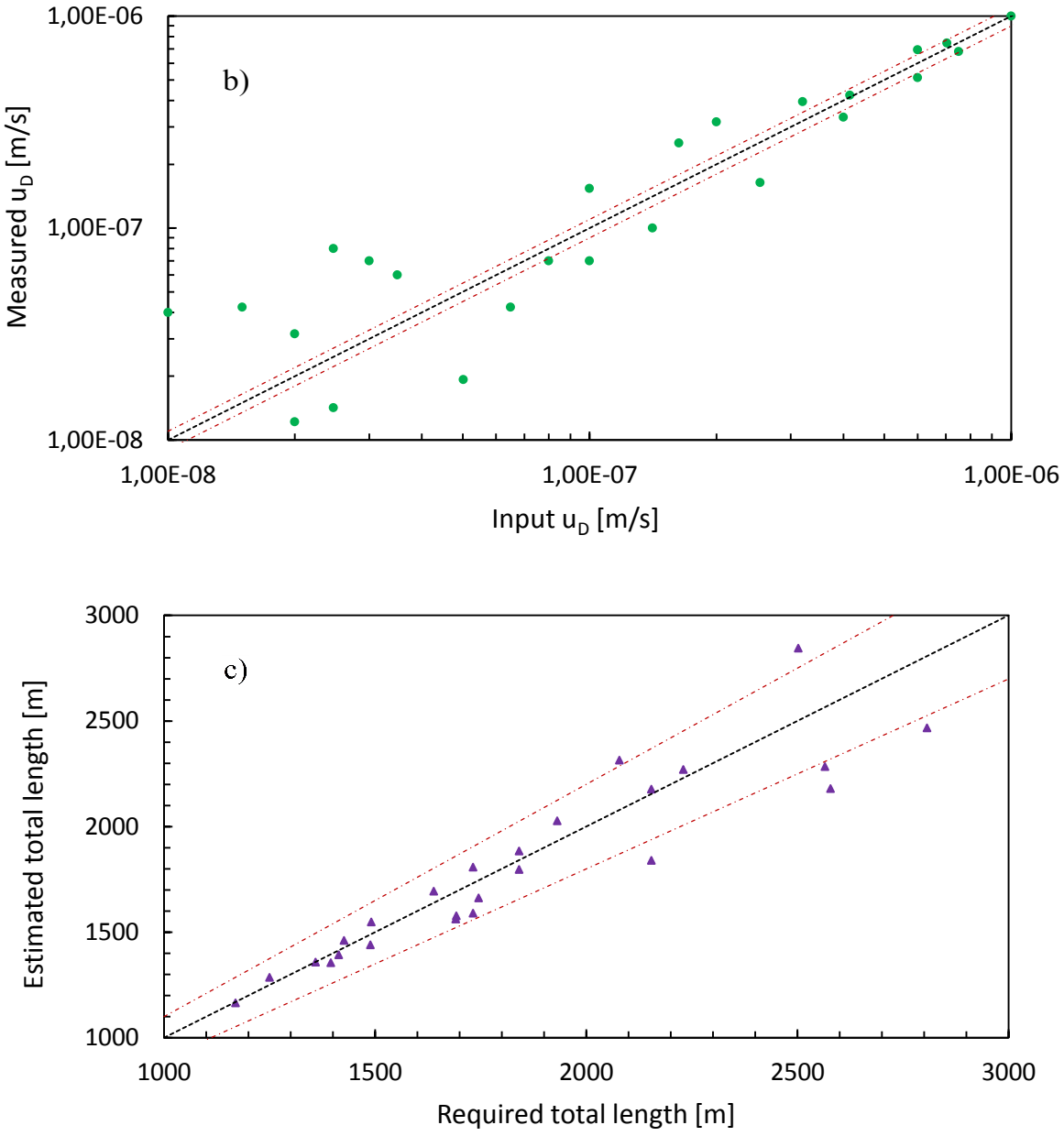

Figure 3.6 – Comparison of the estimated parameters to the real ones for: a) subsurface thermal conductivity, b) Darcy velocity, and c) the required borefield length (red dashed lines represent an error of ±10%).

The evaluation of the thermal conductivity was very accurate as all estimations fell within a range of ±5% of the true value – the maximal error registered was 3.2%. This is caused by the fact that the error function that is minimized is extremely sensitive to $\tilde{k}$.

The estimation of the Darcy velocity did not show such a high precision. Unless the groundwater flow is very fast $\left(u_D \geq 3\times10^{-7}\,m/s\right)$, the algorithm finds a value for the Darcy velocity that is close to the true value, with an error within ±10%. Estimating the Darcy velocity requires differences of temperature between the sensors that are not easily perceptible by the TRT at low Peclet, especially when considering the thermal sensor uncertainties. Nevertheless, the difficulty of the TRT to identify the correct groundwater flow velocity at low Pe does not impact too much on the required borefield length, since differences with the borefield total length obtained with the exact flow parameter were usually smaller than 10%. It can be observed in Fig. 3.6c that at high required total length, some points slightly fall outside of the red lines defining the ±10% of difference between required length evaluated with real parameters and estimated ones. These points corresponds to situations of low conductivity and medium flow velocity, for which advection, even though difficult to measure with a short-term test can become significant compared to conduction on the long-term and thus, can affect the required length.

Figure 3.7 illustrates the error on required borefield length when neglecting groundwater flow during the design process as a function of Peclet (red line), compared with the results obtained in Fig. 3.6. The red line was obtained by calculating, for multiple flow velocities, the error in design when a Darcy velocity of zero is assumed according to the abovementioned borehole sizing model. A constant thermal conductivity of 4.8 W/mK was used in these calculations and it was assumed that its measurement was exact. Therefore, the overdesign shown by the red line in Fig. 3.7 is strictly caused by neglecting advection. For the cases tested, at low Pe (<0.01), using the resulting ground parameters from the H/TRT (diamond symbols) can lead to a small underestimation of the correct required length (i.e. the one calculate with the true ground parameters). For some of these cases at low Pe, the required length "misdesign" was actually more important that the one obtained when neglecting groundwater flow in the design procedure. It might be preferable to simply neglect groundwater flow when $Pe \leq 0.005$ in order to prevent this. However, at moderate and high Pe, accounting for groundwater flows with the proposed H/TRT

provided a much better sizing of the geothermal borefield compared to neglecting groundwater. At Pe = 0.1, the borefield overdesign when neglecting advection is 74.9% for the case tested. Using the H/TRT and the methodology described in this paper, the error on the required length of the geothermal wells is more limited, with maximal misestimation of 13.7%.

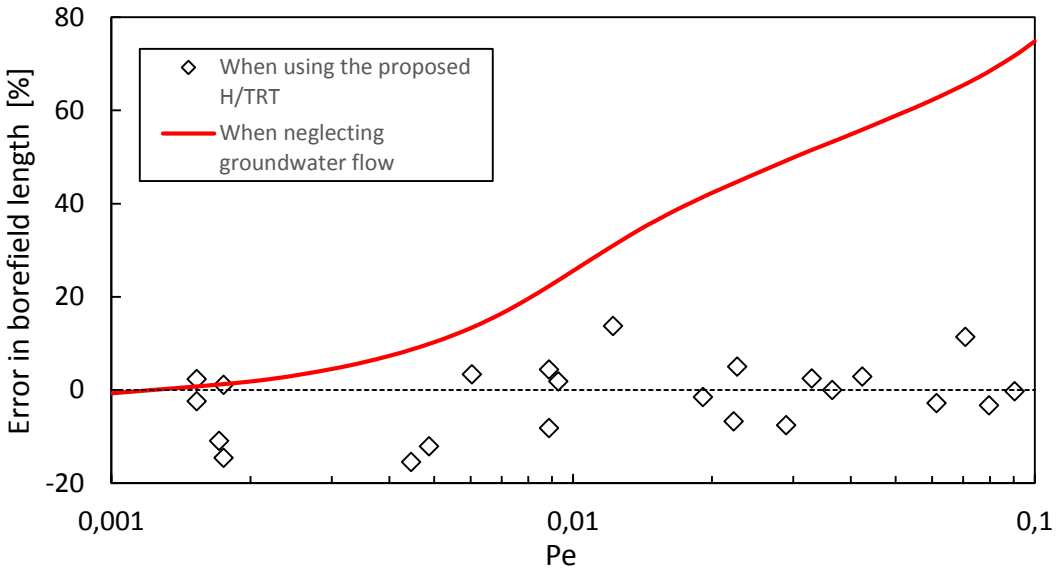

Figure 3.7 – Comparison of the error on the required total GHE length induced by the H/TRT apparatus with the one induced by entirely neglecting advection.

Unless water flows at an extreme velocity, the effective ground thermal conductivity measured by TRT should be nearly equal to the true thermal conductivity. Eq. (3.9) shows that advection effects increase with time and thus, advection may not be important enough to alter the measurements of TRTs considering their relatively short duration. As a result, errors in borefield length caused by traditional tests where the flow is not considered should follow the red line in Fig. 3.7. To verify this, simulations of 3 days of heating in different geological environments were done after which the ground thermal conductivity was calculated from the line source method. Table 3.3 shows that within the range of Peclet studied in this paper (≤ 0.1), the line source method provides approximately the same value of thermal conductivity for all flow velocities. The effective thermal conductivity changed only when $\mathrm{Pe} > 0.1$, which is out of the scope of this work.

As a reminder, depending on the ground properties, such a Peclet number corresponds to a scale of Darcy velocity of $u_D \sim 10^{-6} m/s$.

Table 3.3 Effective thermal conductivity calculated from the line source method for different flow velocities.

Flow Peclet number Pe [-]	Measured effective thermal conductivity k_{eff} [W/mK]
0.001	4.58
0.005	4.58
0.01	4.58
0.05	4.59
0.1	4.62
0.5	6.40

Finally, it is instructive to evaluate the performance of the approach proposed in this paper as a function of the heat generation rate of the source and of the uncertainty of the temperature probes. Low power input allows cheaper TRTs, but leads to smaller observable temperature differences between probes. Also, accurate temperature sensors are more expensive. Table 3.4 illustrates the effects of the injection rate and temperature measurement uncertainties on the reliability of the estimation procedure. It shows the relative error on the required GHE length for different combinations of heat injection rate and temperature uncertainty, with $\tilde{k} = 8$ and $Pe = 0.01$. As a reminder, this setting corresponds to one of the most detrimental situation for the H/TRT performance, when groundwater flow is low enough to be hard to detect, but high enough to have an impact on the borefield sizing. It should be noted that due to the randomness of the array ω, Table 3.4 only provides a general idea of the effects of uncertainties and no statistical analysis is attempted here. While the evaluation of $\tilde{k}$ remains relatively good in all cases, high noise on the temperature measurements causes a loss of accuracy for the evaluation of the groundwater flow parameters. In the three situations where sensors have an uncertainty of $\pm 0.5°C$, the relative errors on the flow velocity were –90.0% $\left(q_0' = 20 W/m\right)$, –91.1% $\left(q_0' = 40 W/m\right)$ and 122% $\left(q_0' = 80 W/m\right)$. On the other hand, sensors that have great accuracy (±0.01°C) offers a better estimation, as long as there is enough heat coming out

of the source. With $q'_0 = 40 W/m$ and $q'_0 = 80 W/m$, the measured Darcy velocity was $2.4 \times 10^{-7} m/s$, which represents an overestimation of 4.8% of the true value. For $q'_0 = 20 W/m$, the source was not strong enough to generate variations of temperatures between the probes in spite of their great precision. Consequently, the solver underrated by 76.9% the flowrate of groundwater, hence the suggestion to employ power input superior or equal to ~40 W/m for the H/TRT.

Table 3.4 Resulting estimation of parameters for various scenarios. (true values are $\tilde{k} = 8.00$, Pe = 10^{-2} and $\phi = 33°$).

Heat generation rate q_0 [W/m]	Temperature sensors absolute uncertainty [°C]	Estimated ratio of thermal conductivities $\tilde{k}$ [-]	Estimated flow Peclet number Pe [10^{-2}]	Estimated ground thermal conductivity k_{avg} [W/mK]	Estimated Darcy velocity U_D [10^{-7} m/s]
	0.01	8.00	0.23	4.78	0.5
20	**0.1**	8.09	0.61	4.84	1.4
	0.5	8.05	0.10	4.81	0.2
	0.01	8.06	1.0	4.82	2.4
40	**0.1**	8.07	0.84	4.83	1.9
	0.5	8.11	0.10	4.85	0.2
	0.01	8.06	1.0	4.82	2.4
80	**0.1**	8.09	0.99	4.84	2.3
	0.5	8.12	2.2	4.85	5.1

3.6 Conclusions

The purpose of this paper was to analyse the possibility to apply inverse heat transfer techniques to a H/TRT concept that uses an electric cable and temperature probes to simultaneously measure the ground hydraulic and thermal properties. It is possible to execute it at various depths to find the distribution of ground properties, leading better sized ground heat exchangers. Knowing groundwater flow properties is important during the design process of geothermal fields. Although the idea of H/TRT had been numerically validated before, the configuration studied in this paper was modified to ease the application of the concept. The perimeter of the borehole is considered impermeable and the heat source has been moved from the center of the borehole to its perimeter. A numerical model was developed to simulate the hydro-thermal response test for various

values of ground thermal conductivity, groundwater flow velocity and orientation, heat injection rate, borehole radius and duration of the heating period.

The present work has demonstrated numerically that it is possible to minimize the error between measured temperatures during the test and temperatures achieved by the model to find the desired properties. A sensitivity analysis revealed that the thermal response test is extremely sensible to the ground thermal conductivity. In part for that reason, the solving procedure is easily able to measure this parameter. However, the thermal response of the proposed concept is less sensitive to the groundwater flow. The flowrate is estimated via the differences of temperatures read by the three sensors. In some cases, these variations of temperatures are small, making it difficult to appropriately evaluate the velocity. Flow orientation can be calculated separately by merely comparing the temperatures of each probe.

Using a typical application, estimated and real ground parameters were translated into a total borefield required lengths. This work showed that using ground parameters obtained from the H/TRT leads to error in sizing of less than 15%, whereas neglecting groundwater flow can yield much larger sizing error, ~80%.

The solution to the inverse heat transfer problem could have been improved with the use of regularization or with another minimization algorithm. Here, only one strategy was tested to demonstrate the potential of the approach. It could be interesting to compare results coming out of this strategy with the ones coming out of other algorithms, such as the Levenberg-Marquardt method or the conjugate gradient method with adjoint problem. The numerical model built for this study was two dimensional. The lack of a third dimension assumes certain hypothesis. While these hypothesis are considered as acceptable, more research about their effects have to be done. For example, there was no axial heat transfer in the model – higher energy generation could be needed when there is. The suggested concept also needs to be tested in-situ and experimentally validated. Fixing the temperature sensors and the electric cable at the desired locations is a manipulation that will not be easily achieved in the field and asks for reflections. Study on the errors propagation created by a wrong positioning of the materials would be of interest.

Chapitre 4 Conclusion

Dans la littérature, on remarque que de plus en plus de modèles de conception de champs d'échangeurs de chaleur géothermique verticaux considérant l'impact des écoulements souterrains sont présentés, mais qu'il y a encore très peu de tests de réponse thermique développés offrant aux ingénieurs une mesure de la vitesse et l'orientation de ces écoulements. Bien qu'il existe des tests en hydrogéologie qui sont capables de mesurer l'écoulement d'eau dans le sol, ceux-ci ne donnent pas d'informations sur les propriétés thermiques du sol; un autre test (de type thermique) est donc nécessaire. Ainsi, le projet de maîtrise avait comme objectif de mettre en place et de valider numériquement un concept de test de réponse thermo-hydraulique mesurant à la fois la conductivité thermique du sol et les paramètres de l'écoulement d'eau souterraine qui s'y écoule. Il s'agit de placer un câble électrique, dégageant de la chaleur dans un puits d'eau, entouré de trois capteurs de température. Pouvoir combiner toutes ces manipulations en un unique test effectué dans un seul forage permet de diminuer autant les coûts reliés aux mesures, que le temps requis.

Les travaux présentés dans ce mémoire et réalisés dans le cadre des activités de recherche à la maîtrise ont permis l'atteinte de cet objectif. Pour y parvenir, deux sous-objectifs ont été défini. Dans un premier temps, il fallait concevoir un modèle numérique simulant la réponse thermique du concept étudié dans un puits situé dans une aquifère où il y a présence d'écoulements souterrains. Ce modèle fut bâti sur un logiciel commercial basé sur la méthode des éléments finis. Dans le but de limiter les temps de calcul et par le fait même de réduire la durée d'une simulation, il n'était que bidimensionnel. Il a été jugé que négliger la dimension verticale du puits était acceptable, autant dans le contexte de transferts thermiques que dans celui hydraulique. Avec le modèle, il a été possible de

simuler un test de réponse thermique en fonction de nombreux paramètres : conductivité thermique du sol, vitesse d'écoulement de l'eau, direction de l'écoulement, puissance de chauffage employé, durée du test, rayon du puits, disposition des capteurs de température, etc. Après quelques simulations, il devint évident qu'à partir d'une certaine vitesse, l'écoulement d'eau atteignant le puits influençait suffisamment le transfert de chaleur à travers le puits pour nettement modifier la réponse thermique du montage. Cela signifiait qu'il était bel et bien possible de mesurer la vitesse et l'orientation des écoulements souterrains à partir du test proposé, en plus d'obtenir une estimation de la conductivité thermique du sol.

Une fois cette constatation faite, une méthode de résolution a dû être conçue pour traduire ces variations de la réponse thermique dans le puits à des estimations acceptables des paramètres recherchées; cela représentait le second objectif secondaire du projet. Deux démarches ont découlés des travaux derrière ce mémoire et sont présentées dans le texte. La première emploie une méthode de plan pour trouver l'orientation de l'écoulement et des techniques graphiques pour mesurer la vitesse de l'eau et la conductivité thermique du sol. La méthode de plan est déjà utilisée par les hydrogéologues, qui estiment la direction d'un écoulement souterrain en construisant un plan à partir de la mesure de la tête hydraulique à trois points différents. La même manipulation est possible avec trois mesures de température. La vitesse et la conductivité thermique peuvent être évaluées par ajustement de courbe. Le processus proposé par la première méthode de résolution est itérative, mais il converge très rapidement. En général, un maximum de trois itérations est nécessaire. Cette démarche offre des mesures assez précises dans des délais rapides, mais elle n'est pas vraiment adaptable, malgré l'emploi de variables adimensionnelles : elle ne fonctionne que lorsque la source de chaleur est fixe au centre du puits, ce qui peut s'avérer compliqué à mettre en place en pratique.

La seconde méthode étudiée applique des techniques de résolution de problèmes de transfert thermique inverses au test de réponse thermo-hydraulique. Il s'agit ainsi d'une approche numérique qui tente de minimiser une fonction erreur à l'aide d'un algorithme d'optimisation. Cet algorithme a pu être choisi à partir du *Optimization Toolbox* du logiciel Matlab. Pour simplifier le travail de l'algorithme, l'orientation a été estimée par la méthode de plan qui est utilisé par la première démarche. L'emploi des concepts de problèmes

inverses s'effectue ainsi sur seulement sur deux paramètres au lieu de trois; cela réduit grandement les temps de calcul et améliore la précision des mesures. Par rapport à la première démarche introduite dans le mémoire, l'approche du problème inverse nécessite un temps d'analyse des données de quelques heures et demande la possession des logiciels numériques nécessaires, mais elle offre une meilleure polyvalence car elle peut être appliquée avec n'importe quelle configuration. Cela fait en sorte que dans la possibilité où le concept de test de réponse thermo-hydraulique étudié soit appliqué sur le terrain, il pourrait être préférable de l'utiliser.

Maintenant que le concept a été validé numériquement et que deux démarches distinctes ont été créées, la prochaine étape majeure de la poursuite de la recherche est de l'essayer expérimentalement, soit un test réel sur le terrain ou un essai dans un montage à échelle réduite. Toutefois, d'autres pistes de recherche peuvent se faire numériquement. On peut penser au fait d'avoir négliger la troisième dimension. Malgré le fait que cela a été jugé comme étant acceptable, il se pourrait que, sous certaines conditions, les vecteurs du flux thermique ou de l'écoulement souterrain aient une dimension verticale. La convection naturelle pourrait particulièrement être forte lorsque l'écoulement est faible. De plus, s'il y a des conditions artésiennes ou de recharge vers le bas, l'écoulement souterrain peut avoir un gradient vertical sans nécessiter de convection. Tous ces phénomènes n'ont pas été considérés. L'algorithme employé par la seconde démarche pourrait être approfondi en appliquant différents concepts de problèmes inverses. Le cas échéant, il faudrait s'attendre à des mesures plus précises dans des délais plus courts. Un important problème qui n'est toujours pas résolu est la manière d'installer en pratique des capteurs de température et une source de chaleur à une position angulaire précise dans un puits restreint et ce, plusieurs mètres sous nos pieds. Une étude sur l'impact d'un mauvais positionnement de l'instrumentation serait d'intérêt.

En somme, malgré qu'il reste des obstacles à contourner, le mémoire montre le potentiel du concept étudié. Il est possible d'observer les écoulements souterrains avec des capteurs de température situés dans un puits et d'y soutirer des estimations justes de la conductivité thermique du sol, de la vitesse des écoulements et de leur direction et ce, malgré la présence d'incertitudes sur la mesure de la température.

Bibliographie

[1] Majorowicz Jacek and Minea Vasile, “Geothermal energy potential in the St-Lawrence River area, Québec,” *Geothermics*, vol. 43, pp. 25–36, Jul. 2012.

[2] M. Malo, F.-A. Comeau, K. Bédard, R. Lefebvre, and R. Therrien, “Assessing the geothermal potential of the St. Lawrence Lowlands sedimentary basin in Quebec, Canada,” *International Association of Hydrogeologists*, 2012.

[3] RETScreen International, “Clean Energy Project Analysis : RETScreen Engineering and Cases Textbook, Ground-source Heat Pump Projet Analysis Chapter.",” Minister of Natural Resources Canada, 2005.

[4] J. Raymond, M. Malo, D. Tanguay, S. Grasby, and F. Bakhteyar, “Direct Utilization of Geothermal Energy from Coast to Coast: a Review of Current Applications and Research in Canada,” in *Proceedings, World Geothermal Congress*, 2015.

[5] Geothermal Energy Association, “2013 Geothermal Power: International Market Overview.” Sep-2013.

[6] A. Chiasson and A. O’Connell, “New analytical solution for sizing vertical borehole ground heat exchangers in environments with significant groundwater flow: Parameter estimation from thermal response test data,” *Hvac&r Research*, vol. 17, no. 6, pp. 1000–1011, 2011.

[7] C. K. Lee and H. N. Lam, “Effects of groundwater flow direction on performance of ground heat exchanger borefield in geothermal heat pump systems using 3-D finite difference method,” in *Proceedings of Building Simulation*, 2007, pp. 337–341.

[8] M. Tye-Gingras and L. Gosselin, “Adapting design procedure for vertical ground heat exchangers to consider groundwater flow,” *Renewable Energy (submitted)*.

[9] M. Tye-Gingras and L. Gosselin, “Generic ground response functions for ground exchangers in the presence of groundwater flow,” *Renewable Energy*, vol. 72, pp. 354–366, Dec. 2014.

[10] N. Diao, Q. Li, and Z. Fang, “Heat transfer in ground heat exchangers with groundwater advection,” *International Journal of Thermal Sciences*, vol. 43, no. 12, pp. 1203–1211, Dec. 2004.

[11] N. Kresic, *Hydrogeology and groundwater modeling*, Second Edition. Taylor & Francis Group, 2007.

[12] A. S. Alden and C. L. Munster, “Field Test of the in situ permeable ground water flow sensor,” *Ground Water Monitoring and Remediation*, pp. 81–88, 1997.

[13] H. S. Carslaw and J. C. Jaeger, *Conduction of Heat in Solids*, Second Edition. Clarendon Press, Oxford, 1959.

[14] COMSOL, *COMSOL Multiphysics User’s Guide, Version 4.2*. Stockholm, Sweden.

[15] Canadian GeoExchange Coalition, “The State of the Canadian Geothermal Heat Pump Industry 2011, Industry Survey and Market Analysis.” 2012.

[16] P. Mogensen, “Fluid fo duct wall heat transfer in duct system heat storages,” presented at the International Conference on Subsurface Heat Storage in Theory and Practice, Stockholm, Sweden, 1983, pp. 652–657.

[17] S. Gehlin, “Thermal Response Test method development and evaluation,” Doctoral Thesis, Lulea University of Technology, Lulea, Sweden, 2002.

[18] B. Sanner, G. Hellström, J. Spitler, and S. Gehlin, “Thermal response test–current status and world-wide application,” in *Proceedings world geothermal congress*, 2005, pp. 24–29.

[19] S. Signorelli, S. Bassetti, D. Pahud, and T. Kohl, “Numerical evaluation of thermal response tests,” *Geothermics*, vol. 36, no. 2, pp. 141–166, Apr. 2007.

[20] H. J. L. Witte, “TRT: How to get the right number,” *GeoDrilling International*, vol. 151, pp. 30–34, Apr. 2009.

[21] M. G. Sutton, D. W. Nutter, and R. J. Couvillion, “A Ground Resistance for Vertical Bore Heat Exchangers With Groundwater Flow,” *Journal of Energy Resources Technology*, p. 183, 2003.

[22] N. Diao, Q. Li, and Z. Fang, “Heat transfer in ground heat exchangers with groundwater advection,” *International Journal of Thermal Sciences*, vol. 43, no. 12, pp. 1203–1211, Dec. 2004.

[23] A. D. Chiasson, S. J. Rees, and J. D. Spitler, “A preliminary assessment of the effects of groundwater flow on closed-loop ground source heat pump systems,” *ASHRAE Transactions*, vol. 106, no. 1, pp. 380–393, 2000.

[24] H. J. L. Witte and G. J. Gelder, “Geothermal response tests using controlled multipower level heating and cooling around a borehole heat exchanger,” presented at the Proceedings of the Tenth Internation Conference on Thermal Energy Storage, New Jersey, USA, 2006.
[25] S. E. A. Gehlin and G. Hellström, “Influence on thermal response test by groundwater flow in vertical fractures in hard rock,” *Renewable Energy*, vol. 28, no. 14, pp. 2221–2238, Nov. 2003.
[26] J. Raymond, R. Therrien, L. Gosselin, and R. Lefebvre, “Numerical analysis of thermal response tests with a groundwater flow and heat transfer model,” *Renewable Energy*, vol. 36, no. 1, pp. 315–324, Jan. 2011.
[27] N. Molina-Giraldo, P. Blum, K. Zhu, P. Bayer, and Z. Fang, “A moving finite line source model to simulate borehole heat exchangers with groundwater advection,” *International Journal of Thermal Sciences*, vol. 50, no. 12, pp. 2506–2513, Dec. 2011.
[28] L. Lamarche and B. Beauchamp, “A new contribution to the finite line-source model for geothermal boreholes,” *Energy and Buildings*, vol. 39, no. 2, pp. 188–198, Feb. 2007.
[29] A. Angelotti, L. Alberti, I. La Licata, and M. Antelmi, “Energy performance and thermal impact of a Borehole Heat Exchanger in a sandy aquifer: Influence of the groundwater velocity,” *Energy Conversion and Management*, vol. 77, pp. 700–708, Jan. 2014.
[30] R. Fan, Y. Jiang, Y. Yao, D. Shiming, and Z. Ma, “A study on the performance of a geothermal heat exchanger under coupled heat conduction and groundwater advection,” *Energy*, vol. 32, no. 11, pp. 2199–2209, Nov. 2007.
[31] Y. Nam, R. Ooka, and S. Hwang, “Development of a numerical model to predict heat exchange rates for a ground-source heat pump system,” *Energy and Buildings*, vol. 40, no. 12, pp. 2133–2140, 2008.
[32] J. C. Choi, J. Park, and S. R. Lee, “Numerical evaluation of the effects of groundwater flow on borehole heat exchanger arrays,” *Renewable Energy*, vol. 52, pp. 230–240, Apr. 2013.
[33] J. Acuña, P. Mogensen, and B. Palm, “Distributed thermal response test on a U-pipe borehole heat exchanger,” in *Effstock-The 11th International Conference on Energy Storage. Stockholm*, 2009.
[34] H. Fujii, H. Okubo, M. Chono, M. Sasada, S. Takasugi, and M. Tateno, “Application of optical fiber thermometers in thermal response tests for detailed geological descriptions,” in *Proceedings of Effstock 2009 conference on thermal energy storage for efficiency and sustainability, Stockholm, Sweden*, 2009.
[35] H. Fujii, H. Okubo, K. Nishi, R. Itoi, K. Ohyama, and K. Shibata, “An improved thermal response test for U-tube ground heat exchanger based on optical fiber thermometers,” *Geothermics*, vol. 38, no. 4, pp. 399–406, Dec. 2009.
[36] A. E. Beck, “The use of thermal resistivity logs in stratigraphic correlation,” *Geophysics*, vol. 41, no. 2, pp. 300–309, Apr. 1976.
[37] J. Raymond, G. Robert, R. Therrien, and L. Gosselin, “A novel thermal response test using heating cables,” in *Proceedings of the World Geothermal Congress, Bali, Indonesia*, 2010, pp. 1–8.
[38] J. Raymond and L. Lamarche, “Development and numerical validation of a novel thermal response test with a low power source,” *Geothermics*, vol. 51, no. 0, pp. 434–444, Jul. 2014.
[39] J. Raymond, L. Lamarche, and M. Malo, “Insights from field experiments to conduct thermal response tests with a low power source,” presented at the Proceedings of the 11th Internation Energy Agency Heat Pump Conference, Montréal, 2014, p. 12.
[40] H. N. Lam and C. K. Lee, “Determination of groundwater flow direction in thermal response test analysis for geothermal heat pump systems,” *HVAC&R Research*, vol. 17, pp. 991–999, 2011.
[41] V. Wagner, P. Bayer, G. Bisch, M. Kübert, and P. Blum, “Hydraulic characterization of aquifers by thermal response testing: Validation by large-scale tank and field experiments,” *Water Resour. Res.*, vol. 50, no. 1, pp. 71–85, Jan. 2014.
[42] H. R. Bravo, F. Jiang, and R. J. Hunt, “Using groundwater temperature data to constrain parameter estimation in a groundwater flow model of a wetland system,” *Water Resour. Res.*, vol. 38, no. 8, pp. 28–1, Aug. 2002.
[43] J. Raymond, R. Therrien, and L. Gosselin, “Borehole temperature evolution during thermal response tests,” *Geothermics*, vol. 40, no. 1, pp. 69–78, Mar. 2011.
[44] N. Molina-Giraldo, P. Bayer, and P. Blum, “Evaluating the influence of thermal dispersion on temperature plumes from geothermal systems using analytical solutions,” *International Journal of Thermal Sciences*, vol. 50, no. 7, pp. 1223–1231, Jul. 2011.
[45] T. L. Bergman, A. S. Lavine, F. P. Incropera, and D. P. DeWitt, *Fundamentals of heat and mass transfer*, Seventh. John Wiley & Sons, 2011.

[46] H. J. L. Witte, “Error analysis of thermal response tests,” *Applied Energy*, vol. 109, pp. 302–311, Sep. 2013.
[47] P. Eskilson, “Thermal Analysis of Heat Extraction Boreholes,” Ph.D. Thesis, Lund University, Lund, Sweden, 1987.
[48] V. Wagner, P. Bayer, M. Kübert, and P. Blum, “Numerical sensitivity study of thermal response tests,” *Renewable Energy*, vol. 41, pp. 245–253, May 2012.
[49] S. M. H. Moghaddam and J. H. Barman, “First step towards development of distributed thermal response test using heating cables,” Kungliga Tekniska högskolan, Stockholm, 2015.
[50] H. S. Carslaw, *Introduction to the mathematical theory of conduction of heat in solids*. New York: Dover, 1945.
[51] A. Fic, “A study of the steady-state inverse heat transfer problem of estimating the boundary velocity,” *Numerical Heat Transfer, Part A: Applications*, vol. 45, no. 2, pp. 153–170, Jan. 2004.
[52] M. N. Ozisik and H. R. B. Orlande, *Inverse Heat Transfer: Fundamentals and Applications*. New York: Taylor & Francis, 2000.
[53] M. Li and A. C. K. Lai, “Parameter estimation of in-situ thermal response tests for borehole ground heat exchangers,” *International Journal of Heat and Mass Transfer*, vol. 55, no. 9–10, pp. 2615–2624, Apr. 2012.
[54] S. Erol, M. A. Hashemi, and B. François, “Analytical solution of discontinuous heat extraction for sustainability and recovery aspects of borehole heat exchangers,” *International Journal of Thermal Sciences*, vol. 88, pp. 47–58, Feb. 2015.
[55] J. Zhang, M. Subotic, and F. C. Lai, “Transient and steady natural convection from a heat source embedded in thermally stratified porous layer,” *International Journal of Thermal Sciences*, vol. 49, no. 9, pp. 1527–1535, Sep. 2010.
[56] A. N. Tikhonov and V. Y. Arsenin, *Solution of Ill-Posed Problems*. Washington DC: Winston & Sons, 1977.
[57] *Optimization Toolbox For Use with MATLAB: User’s Guide*, 3rd ed. Natick: The MathWorks, 2004.
[58] R. H. Byrd, J. C. Gilbert, and J. Nocedal, “A Trust Region Method Based on Interior Point Techniques for Nonlinear Programming,” *Mathematical Programming*, vol. 89, no. 1, pp. 149–185, 2000.
[59] R. H. Byrd, M. E. Hribar, and J. Nocedal, “An Interior Point Algorithm for Large-Scale Nonlinear Programming,” *SIAM Journal on Optimization*, vol. 9, no. 4, pp. 877–900, 1999.
[60] R. H. Byrd, R. B. Schnabel, and G. A. Shultz, “Approximate Solution of the Trust Region Problem by Minimization over Two-Dimensional Subspaces,” *Mathematical Programming*, vol. 67, no. 2, pp. 189–224, 1994.